Journal of Wind Engineering and Industrial Aerodynamics, 7 (1981) 145—189

REVIEW AND CLASSIFICATION OF VARIOUS AERODYNAMIC AND HYDRODYNAMIC MEANS FOR SUPPRESSING VORTEX SHEDDING*

M.M. ZDRAVKOVICH

University of Salford, Salford M5 4WT (Gt. Britain)

(Received May 8, 1980; accepted in revised form September 1, 1980)

Summary

A wide variety of aerodynamic and hydrodynamic means for suppressing vortex shedding is classified into three categories in accordance with the phenomenological mechanism of vortex shedding. The three categories are as follows:

(i) surface protrusions, which affect separation lines and/or separated shear layers, e.g. helical strakes, wires, fins, studs or spheres, etc.;

(ii) shrouds, which affect the entrainment layers, e.g. perforated, gauze, axial-rod, axial-slat, etc.;

(iii) nearwake stabilisers, which prevent interaction of entrainment layers, e.g. splitter plates, guiding vanes, base-bleed, slits cut across the cylinder, etc.

Most means in the first two categories are omnidirectional, i.e. they are effective irrespective of the direction of fluid velocity. Some means in the first and all in the third category are unidirectional, i.e. they are effective only for one velocity direction. All means are described in detail and the reasons for their effectiveness explained.

A comparative assessment of effectiveness is attempted and the need for comparative tests of various means under identical model conditions is stressed. The reduction of effectiveness in the post-synchronisation range, at high intensity of turbulence, and due to multi-cylinder interference is emphasised.

1. Introduction

The mechanism of vortex shedding behind a circular cylinder and the oscillations related to it have been studied for more than a century but our understanding is still incomplete [1—4]. The complexity of the phenomena involved is reflected in a distinct variation and almost limitless modification of the flow pattern as affected by the Reynolds number, turbulence level, surface roughness, three-dimensionality, and elastic response, to mention only a few factors.

The Reynolds number effect on a turbulent vortex street can be classified into three regimes:

(i) subcritical regime, within which transition to turbulence occurs in separated shear layers;

*This review forms part of the book, "Flow Around Circular Cylinders", by the same author, currently in preparation.

(ii) critical regime, within which transition to turbulence takes place near the separation point of the boundary layers;

(iii) postcritical regime, characterised by fully turbulent boundary layers before the separation.

Vortex shedding persists throughout the subcritical regime, the Strouhal number being almost constant. The drastic narrowing of the wake at the critical regime, due to the formation of the separation bubble and subsequent delayed turbulent separation, doubles the value of the Strouhal number at first [5]. The irregular transition to turbulence in the boundary layer causes a highly irregular separation line, which seems to prevent vortex formation and shedding within the supercritical range of the critical regime [5]. Regular vortex shedding reoccurs in the postcritical regime [6].

The most striking feature of the subcritical regime is that despite the constancy of the Strouhal number, the pressure fluctuations around the cylinder vary considerably. The closely related fluctuating lift reaches maximum values only in the upper subcritical range, where the formation of vortices takes place immediately behind the cylinder [7]. The fluctuating-lift coefficient is almost negligible in the critical regime, and increases, but remains small, in the postcritical regime [8].

The intensity and scale of the free stream turbulence promotes the transition of the separated shear layers in the subcritical regime and the transition of the boundary layers in the critical regime. The result is a shift of all three regimes towards lower Reynolds numbers [9].

The surface roughness of the cylinder produces similar effects on the transition to turbulence [9]. There is, however, an additional effect, which has a profound influence in the critical regime. The surface roughness induces more regular transition to turbulence and straightens the separation line. The separation bubble and the supercritical range as described above do not exist [10]. Hence vortex shedding does not cease for the rough cylinder [11].

Three-dimensionality represents an important, but often neglected, aspect of the phenomenon. The fluctuations are not correlated along the span of the cylinder for more than a few diameters. A long, nominally two-dimensional cylinder generates a three-dimensional fluctuating flow pattern despite the constancy of time-averaged parameters along its span [12].

The end effects for a finite cylinder are usually confined to within a few diameters near the end when the aspect ratio is high. There is a decrease in the Strouhal number and an increase in the spanwise correlation of fluctuations for low aspect ratios [13]. The efflux from the free-end changes the apparent aspect ratio and consequently the flow pattern.

The last but most important and dramatic effect on vortex shedding is produced by an elastic response of the cylinder. The amplitude of vortex-induced oscillation increases as the vortex shedding frequency approaches the natural frequency of the cylinder. When the synchronisation of these two occurs it persists over a 40—60% increase in velocity. Within the synchronisation range the vortex shedding is fully governed by the cylinder's oscillation,

and the maximum amplitude occurs in the middle of that range [14]. The apparent Strouhal number decreases throughout the synchronisation range and the apparent value at the maximum amplitude is always lower than that measured behind a stationary cylinder.

The oscillation of an elastic or elastically supported cylinder improves remarkably the correlation of fluctuations along the span [12]. Vortex formation takes place nearer to the cylinder surface, and the decrease in the apparent Strouhal number allows longer periods of time for vortex formation. These three effects combined contribute to a significant increase in the fluctuating lift. It has been found that the latter can increase by a full order of magnitude in the upper subcritical range [12], almost two orders of magnitude in the lower subcritical range [7], and can maintain vortex-induced oscillation throughout the critical regime [11], where apparently vortex shedding does not occur when the cylinder is stationary.

Prevention of vortex-shedding-induced oscillations can be dealt with by structural methods, e.g. by increasing either the natural frequency or energy absorption. The former can be accomplished by increasing the stiffness or redistributing the mass, the latter by using various kinds of structural dampers. Walshe and Wootton [15] described tuned, impact, and active mechanical dampers in their excellent review. The second method of preventing oscillations is based on avoiding regular vortex shedding along the cylinder by adopting some aerodynamic or hydrodynamic means. In the discussion that follows, unsuccessful as well as successful types of this method are described, following Walshe and Wootton [15]. More-recent means are also evaluated.

2. Classification of various means

Two novel concepts, an "entrainment layer" and a "confluence point", have been recently introduced and used for the phenomenological explanation of vortex shedding mechanisms and related phenomena [16]. The entrainment layers supply irrotational fluid necessary for the growth of vortices in addition to the rotational fluid, in separated shear layers. The confluence point marks the region where the two entrainment layers coming from the opposite sides of the cylinder meet and interact. The vortices are formed by a rolling-up process and the timing of vortex shedding is governed by the switch of the confluence point from one side of the wake axis to the other. Therefore it should be expected that vortex shedding can be suppressed by interfering with shear layers or entrainment layers, and/or preventing the confluence-point switch.

A wide variety of aerodynamic and hydrodynamic means for suppressing vortex shedding is classified into three categories in accordance with the phenomenological mechanism of vortex shedding. The three categories are as follows:

(i) surface protrusions (strakes, wires, fins, studs, or spheres, etc.), which affect separation lines and/or separated shear layers;

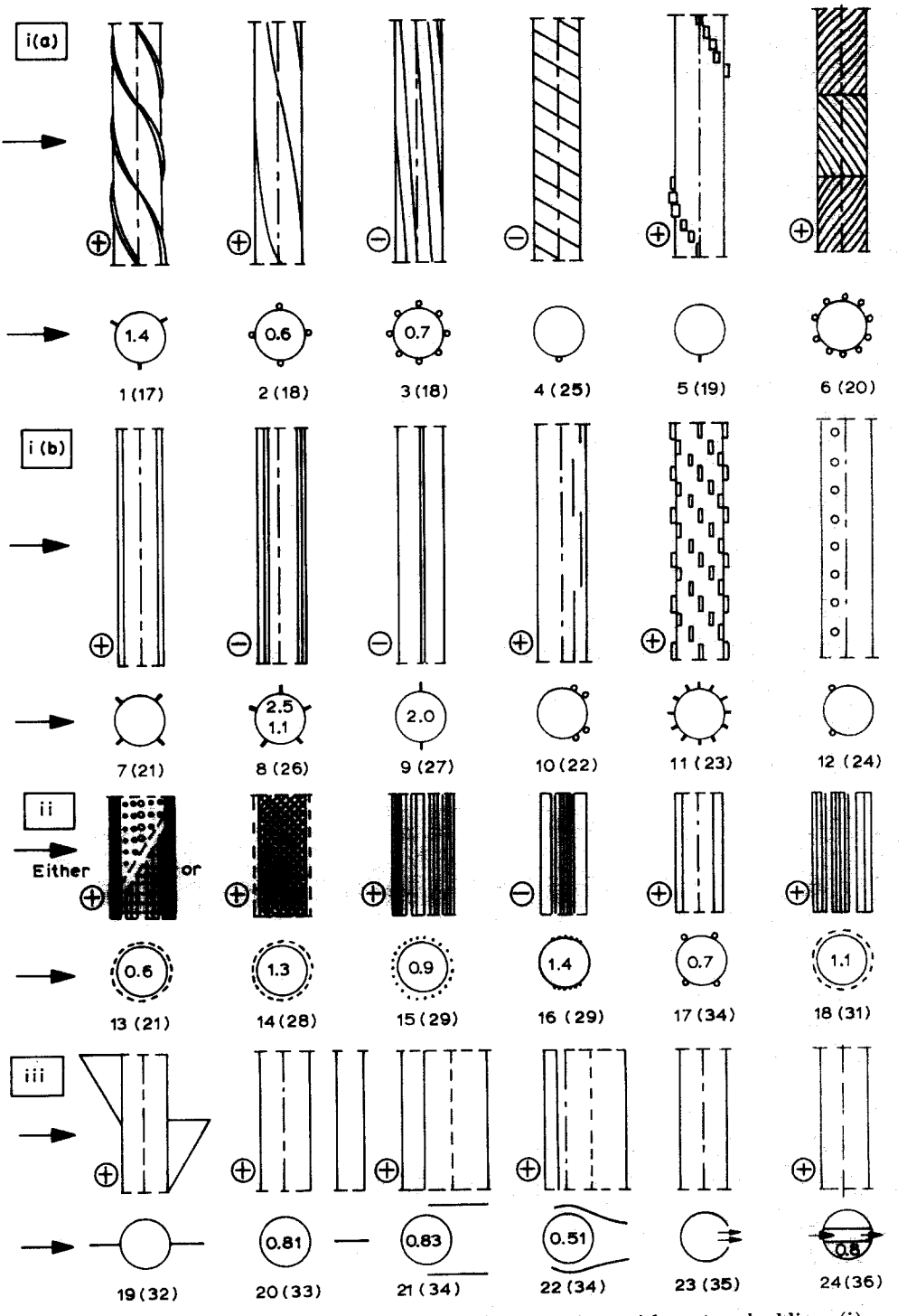

Fig. 1. Aerodynamic and hydrodynamic means for interfering with vortex shedding: (i) surface protrusions ((a) omnidirectional and (b) unidirectional), (ii) shrouds, (iii) nearwake stabilisers (⊕ effective, ⊖ ineffective).

(ii) shrouds (perforated, gauze, axial rods and axial slats, etc.), which affect the entrainment layers;

(iii) nearwake stabilisers (splitter and saw-tooth plates, guiding plates and vanes, base-bleed, slits cut along the cylinder, etc.), which affect the switch of the confluence point.

Figure 1 shows the various aerodynamic and hydrodynamic means grouped into the proposed three categories. The first category, of surface protrusions, was further subdivided into two in order to separate the omnidirectional means from the unidirectional ones. The two subdivisions, with representative types, are:

(a) omnidirectional means, which are not affected by the direction of fluid velocity:

Scruton and Walshe's [17] helical strakes (1957) (**1** in Fig. 1)
Nakagawa et al.'s [18] helical wires (1959) (**2**)
Novak's [19] rectangular plates forming a helix (1966) (**5**)
Sallet and Berezow's [20] helical wires forming a herringbone pattern (1972) (**6**)

(b) unidirectional means, effective only in one direction of velocity as shown in Fig. 1:

Price's [21] four straight fins forming an X cross (1956) (**7** in Fig. 1)
Naumann et al.'s [22] staggered straight wires (1966) (**10**)
Alexandre's [23] staggered rectangular fins (1970) (**11**)
Mizuno's [24] small spheres as turbulence promoters (1970) (**12**)

Slight change in geometry may lead to an *enhancement* of oscillation which exceeds that found for the plain cylinder. These "adverse" means are denoted with a minus sign and they are:

Nakagawa et al.'s [18] eight helical wires (1959) (**3** in Fig. 1)
Nakagawa et al.'s [25] single helical wire (1963) (**4**)
Mahrenholtz and Bardowicks's [26] five straight fins (1978) (**8**)
Gartshore et al.'s [27] symmetric side-fins (1978) (**9**)

The second category covers all possible shapes of shrouds. The full shrouds are omnidirectional but when incomplete they become unidirectional means. The following types of shrouds have been developed:

Price's [21] perforated shroud with circular and square holes (1956) (**13** in Fig. 1)
Zdravkovich and Volk's [28] fine mesh gauze used as a shroud (1972) (**14**)
Zdravkovich's [29] parallel axial rods forming a shroud (1971) (**15**)
Zdravkovich's [30] "shroud" reduced to four rods (1973) (**17**)
Wong's [31] shroud consisting of straight slats (1977) (**18**)

Note that a partial shroud such as that shown in Fig. 1 (**16**) more than doubles the vibrational response in comparison with that of the plain cylinder.

The third category encompasses a wide variety of nearwake stabilisers which

possess only unidirectional effectiveness:

Baird's [32] saw-tooth fins (1955) (19 in Fig. 1)
Roshko's [33] detached splitter plate (1955) (20)
Grimminger's [34] guiding plates (1945) (21)
Grimminger's [34] guiding vanes (1945) (22)
Wood's [35] base-bleed into the nearwake (blunt aerofoil) (1964) (23)
Igarashi's [36] slit along the cylinder (1978) (24)

The extraordinary feature of this category is that there is no disruption of boundary layers either circumferentially or in a spanwise direction. The entrainment either across or into the nearwake is affected in such a way as to postpone vortex shedding further downstream.

3. Surface protrusions

3.1 Mechanism of turbulence promotion

Prandtl [37] demonstrated that an artificial turbulence can be "tripped" in the boundary layer by a wire fixed around a sphere. Small drag coefficients typical for critical Reynolds numbers are then obtained even with fairly low Reynolds numbers.

Fage and Warsap [9] made a detailed study of the effect of a tripping wire attached to a circular cylinder on prematurely promoting the critical regime. They selected five sizes for this wire such that the ratio of the wire diameter to the average thickness of the boundary layer ranged from 0.03 to 0.57, so that each of the wires was totally immersed in the laminar boundary layer. Fage and Warsap's original plot of drag measurements is reproduced in Fig. 2, for wires attached at ± 65° from the stagnation point. It is evident that the shape of the drag curve undergoes a regular change as the diameter of the wires increases; even the finest wires, which displaced only 3% of the boundary layer thickness, had a large effect. Fage and Warsap noticed that the disturbance created by the tripping wires becomes less severe when they are moved upstream towards the stagnation point. They found that tripping wires placed at ±25° had practically no effect, except locally on the pressure distribution around the circular cylinder.

James and Truong [38] carried out similar measurements by attaching a single tripping wire. Figure 3 illustrates the change of drag coefficient with the Reynolds number for various circumferential locations of the tripping wire having $d/\delta = 1$. Again, the location at 65° seems to be the most effective, but with considerable increase of the drag coefficient in the lower subcritical range. A lift coefficient of ~0.5 was found for the optimal position of the tripping wire.

Price [21] carried out free-vibration tests in a water channel at $Re = 4.64 \times 10^3$ for a very lightly spring-restrained cylinder fitted with three tripping wires at 0 and ± 60° having diameters* of $0.023D$. The maximum amplitude of vibration was $2.5D$, the same as found for the plain cylinder. The same

*D throughout this paper refers to the cylinder diameter.

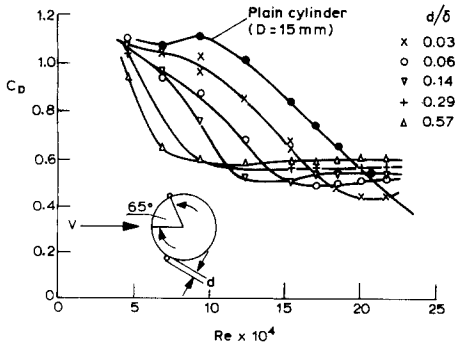

Fig. 2. Effect of size of tripping wires on drag coefficient (after Fage and Warsap [9]).

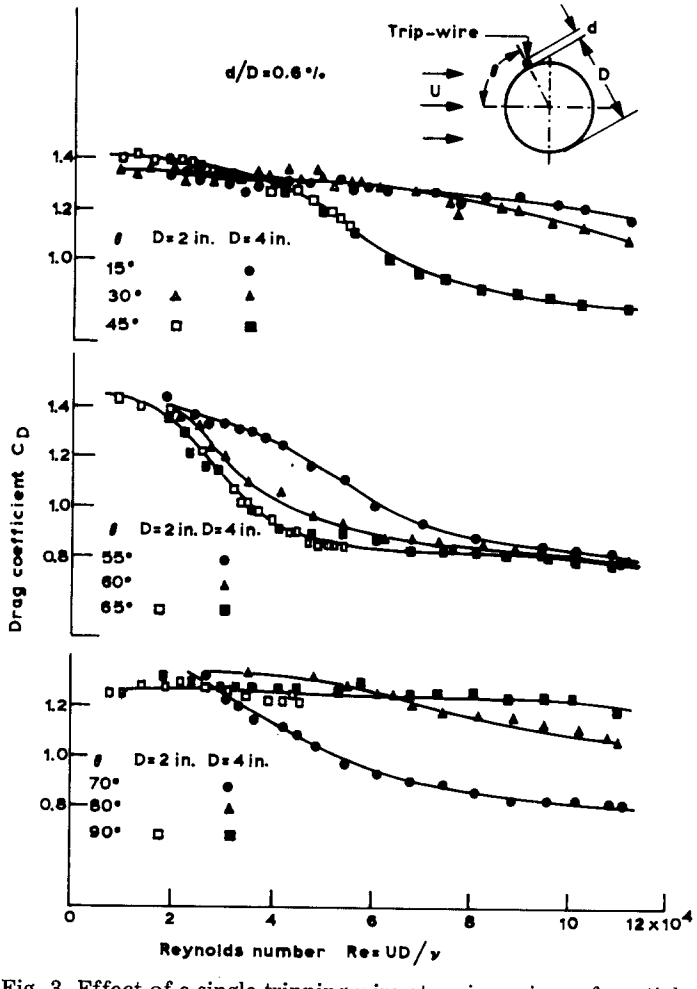

Fig. 3. Effect of a single tripping wire at various circumferential positions on drag coefficient (after James and Truong [38]).

three wires wound helically around the cylinder with a pitch of $20D$, reduced the maximum amplitude only to $1.5D$. Price concluded that neither straight tripping wires nor the most effective helical ones were effective in suppressing large-amplitude vibration and he diverted his research to perforated shrouds, which will be described in Section 4 below.

3.2 Helical strakes

Scruton and Walshe [17] developed efficient surface protrusions for avoiding wind-excited oscillations of cylindrical structures. Three strakes of sharp-edged rectangular section were wound as three helices around the surface of the cylinder, with a pitch of $15D$ (see Fig. 1, 1). It was found that the attachment of quite a low strake, $h = 0.029D$, was effective in reducing the aerodynamic excitation, as can be seen from Fig. 4. Some small improvement was effected by making $h = 0.059D$, with a notable shift of the critical velocities as seen in Fig. 4. Further increase to $0.088D$ was accompanied by a further increase of the critical reduced velocity at which maximum amplitude occurred and by a marked reduction in the area of the instability region, Fig. 4. Finally, with $h = 0.118D$, the instability region was reduced to such a small area that only a small structural damping was necessary to suppress the oscillations. The tests were discontinued at this stage since the small remaining area of instability was not considered to be of practical significance*.

Woodgate and Maybrey [39] carried out tests to determine the optimum pitch for the three strakes. The outcome was a reduction of the pitch from the original $15D$ to $5D$, whilst the height of the strakes remained at $0.09D$ (except for light or lowly damped structures, for which they advised an increase in height to $0.12D$). The effectiveness of the system was not impaired by a gap of $0.005D$ between the strake and the cylinder surface. It has been proved sufficient to apply strakes only to the top third of a chimney stack to prevent instability in the fundamental mode (the general principle is to apply strakes in the region of antinodes).

Cowdrey and Lawes [40] measured the drag coefficient of a cylinder fitted with the helical strakes. The drag coefficient was found to be almost constant from the high subcritical regime ($\mathrm{Re} = 1 \times 10^5$), through the critical regime up to the postcritical one ($\mathrm{Re} = 4 \times 10^6$). This implies that the same flow pattern persists throughout that Reynolds number range. The values of the drag coefficients measured for two heights of the strakes, $0.06D$ and $0.12D$, were found to be 1.35 and 1.45, respectively. These values are high, particularly in the critical regime where the plain cylinder had a drag coefficient of less than 0.5.

Some further tests on the helical strakes were carried out by Ruscheweyh [41], confirming that the optimal pitch is between $4D$ and $5D$ and that only

*The Reynolds number for these tests was not given, but it is inferred that it was within the 1×10^5—1×10^6 range.

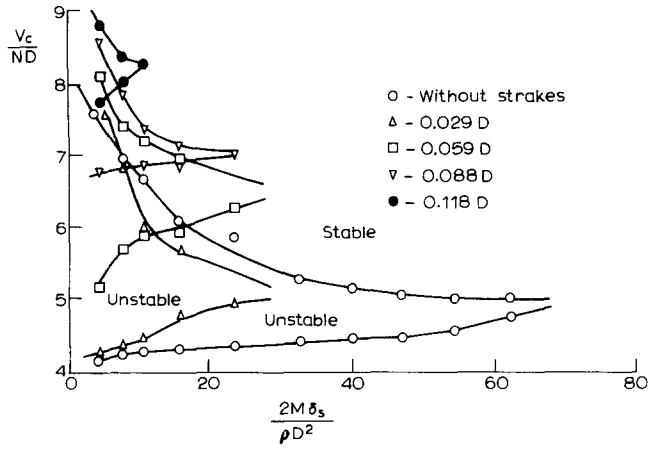

Fig. 4. Effect of height of strakes on the aerodynamic instability of a two-dimensional circular cylinder (after Scruton and Walshe [17]).

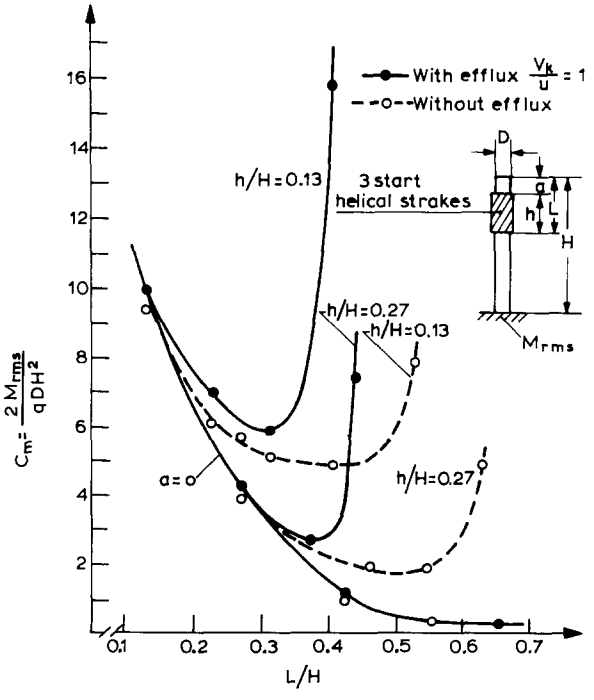

Fig. 5. Effect of efflux and tip distance on effectiveness of strakes (after Ruscheweyh [41]).

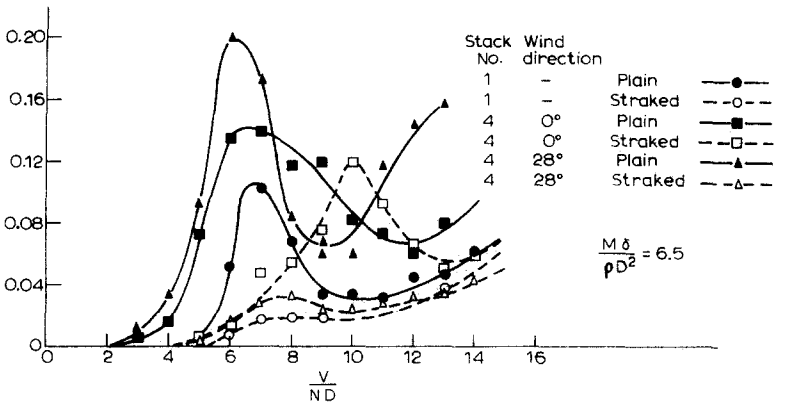

Fig. 6. Variation of amplitude with reduced velocity for the fourth cylinder in a line of four (after Vickery and Watkins [42]).

1/3 of the height should be covered for the Reynolds number range from 1.8×10^4 to 4×10^4. The effect of lowering the area covered by strakes from the top of the chimney towards its base can be seen in Fig. 5. The measured moment at the base of the model is shown versus the relative lowering of the straked area. The latter has a small effect at first, but when the top uncovered part is equal in height to the covered area the effectiveness is severely impaired. An efflux had a further destabilising effect on the effectiveness of the strakes.

Walshe and Wootton [15] pointed out that the effectiveness of helical strakes may be reduced if the stack is supporting an external pipe of small diameter parallel to its axis. The benefit derived by fitting the helical strakes is dependent on the particular configuration and this was assessed in their wind tunnel tests.

Vickery and Watkins [42] carried out tests in water and found that helical strakes were as effective as they were in air in suppressing oscillations of a single cylinder. The wind tunnel tests on a group of four plain and straked cylinders revealed that the addition of strakes was less effective in reducing the amplitudes of vibration of downstream cylinders. Figure 6 shows the variation of the amplitude of vibration with the reduced velocity. The single-cylinder results are reproduced for a comparison with the fourth cylinder in the line. The latter underwent the most severe vibrations when positioned at 28°, and the helical strakes were fully effective for that arrangement. Large vibrations also occurred when the fourth cylinder was in line with the others, and were suppressed at the critical reduced velocity. At a higher reduced velocity of 10, however, the helical strakes became ineffective. The reason for this was not known and all additional modifications, like using left-hand helices on stacks 1 and 3, removal of one strake from each cylinder to produce an asymmetric arrangement, an increase of pitch to $7.5D$, a decrease of pitch to $2.8D$, and an increase of strake height to $0.22D$, were unsuccessful.

Finally, Gartshore et al. [27] noticed an unexpected effect of free-steam turbulence on the effectiveness of the three helical strakes. The tests were carried out in a wind tunnel on a two-dimensional, elastically supported model*, and the results presented in terms of the ratio of the maximum r.m.s. deflection of a model fitted with strakes to the maximum r.m.s. amplitude of the plain cylinder. When the model was submerged in a smooth flow the helical strakes reduced the amplitude of vibration at the critical velocity by a factor of ~100. The maximum response, at the elevated reduced velocity of 8, decreased in amplitude by a factor of 18.

Unexpectedly, the effectiveness of helical strakes diminished when the cylinder was submerged in a turbulent flow (14% intensity). The maximum amplitude of vibration of a plain cylinder was about half that found in smooth flow, but the helical strakes reduced this amplitude by only a factor of 5. At the elevated reduced velocity of 8, the reduction factor was only 2. The important conclusion drawn was that the effectiveness of strakes decreases with the intensity of turbulence of the free stream and with increasing reduced velocity for a model having the same damping. The latter aspect will be discussed in more detail in Section 4 below.

3.3 Helical wires

An additional insight into the interplay and fine balance of the various mechanisms involved in the operation of helical strakes may be gained by describing successful and unsuccessful helical wires.

Nakagawa et al. [18] carried out tests in a huge open-jet wind tunnel on a flexibly mounted cylinder, at supercritical Reynolds numbers. The models oscillated at their natural frequencies throughout the supercritical range and the maximum response was found not only around reduced velocities of 5 to 6 but also at multiples and submultiples of the critical value. The remarkable feature was that the response increased in amplitude and became confined within a narrower band of velocities when the free stream turbulence was increased.

The most striking feature was that a winding of eight thin wires (Fig. 1, 3) having only 0.4% of the cylinder diameter doubled the maximum amplitude of vibration compared to that of the plain cylinder. Reduction of the pitch to $0.5D$ by winding only one wire around the cylinder (see Fig. 1, 4) produced vibrations of the same magnitude as those found on the plain model in turbulent flow [25]. The use of four wires at a pitch of either $8D$ or $16D$ had a magic effect of suppressing oscillations throughout the tested range, as can be seen in Fig. 7.

Nakagawa et al. also measured the drag coefficients; the values are shown within each circle in Fig. 1. The successful four-wire means had a drag coefficient less than that of the unsuccessful one, which would be expected if vortex

*The Reynolds number was not stated but it might be inferred that it was well within the subcritical regime.

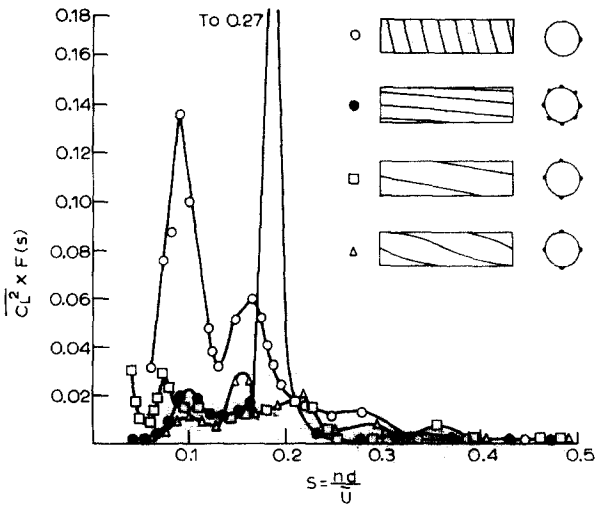

Fig. 7. Power spectra of lift forces for cylinders with helically wound wires (after Nakagawa et al. [18,25]).

shedding was suppressed. Surprisingly, the drag coefficient is less than half that produced by three strakes. Walshe and Wootton [15] argued that sharp-edged rectangular strakes were more effective than those of circular or any other rounded section.

The other puzzling aspect was that the optimum pitch (8—16*D*) found for four helical wires is far away from that (4—5*D*) obtained for three rectangular strakes. Weaver [43] carried out further experiments with helical wires in order to find an optimum number, size, and pitch of windings and the minimum portion of the model which must be covered. Figure 8(A) shows the influence of the number of windings on the effectiveness of reducing the lift force measured on stationary models. The maximum reduction of the fluctuating lift force is found for four wires, although three wires are equally efficient. Nakagawa's and Scruton's values were confirmed.

The influence of the wire diameter on the effectiveness of suppression is shown in Fig. 8(B). The circular wire displays similar characteristics to the rectangular strakes employed by Scruton and Walshe [17]. Figure 8(C) shows a small influence of pitch on the effectiveness within the range 8—16*D*. Note a steep rise of all curves for higher pitches, which should be expected from Nakagawa's results for eight wires at a pitch of 64*D*. Six helical wires were tested by Price [21] and found to be ineffective for all pitches within the range 0.5—20*D*.

Figure 8(D) reveals the effect of the percentage area covered with helical windings on the effectiveness in reducing the amplitude of vibration. The characteristic shift of the maximum response towards high reduced velocities

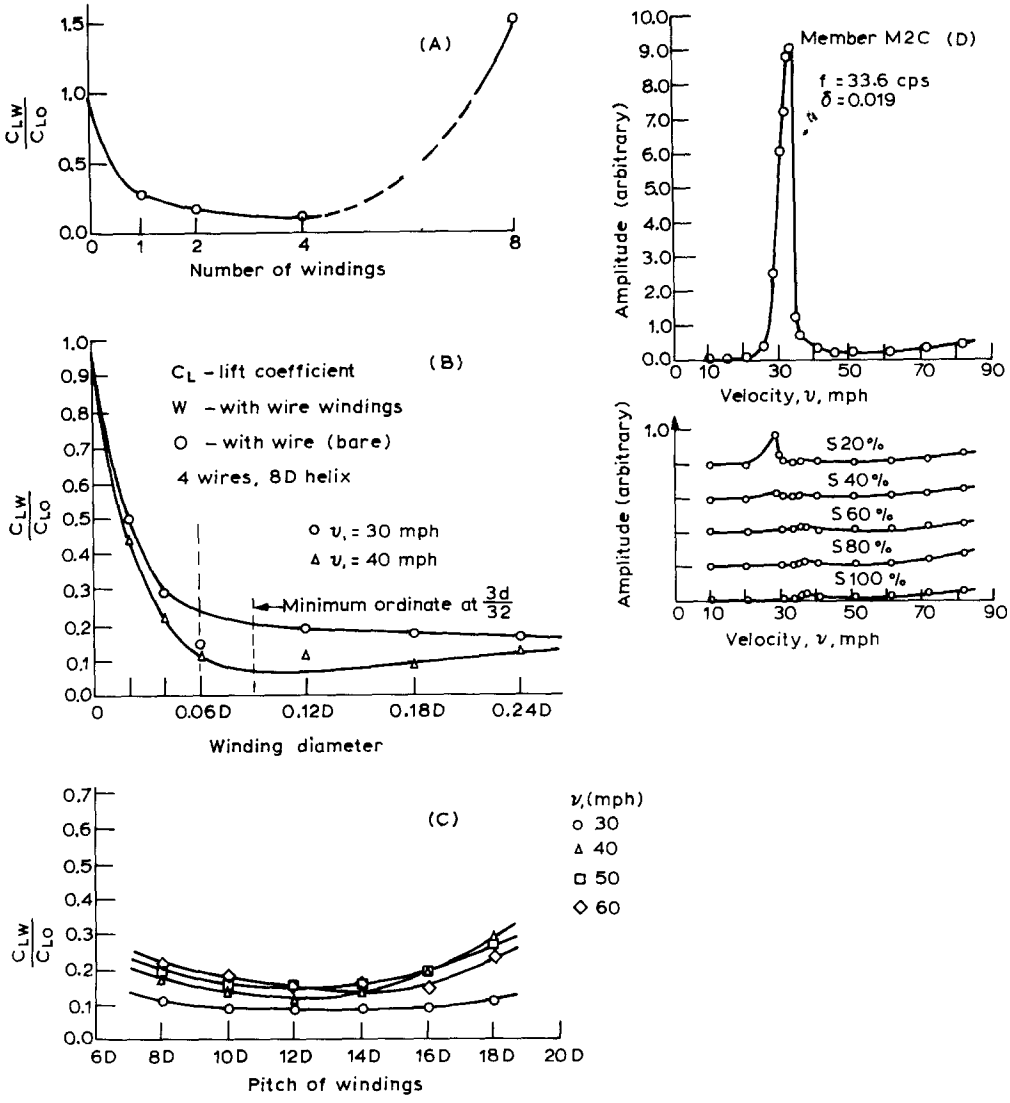

Fig. 8. Effectiveness of helically wound wires: (A) effect of number of wires, (B) effect of wire size, (C) effect of wire pitch, and (D) effect of coverage area (after Weaver [43]).

occurs somewhere between 40 and 60%. Hence it seems that the minimum recommendable coverage should be 50% of the total height of the stack, which is greater than the required coverage of 33% for three helical strakes [17]. It should be mentioned that Nakagawa et al. [25] fitted four cables along the entire length of a stack in Sakai, Japan.

3.4 Helical "variations"

There have been two interesting attempts to increase three-dimensionality along the span of the cylinder not by helical windings *per se* but with additional discontinuities in the helix itself. The same basic concept resulted in two entirely different designs. Novak [19] proposed* to form a helix by fitting small rectangular plates at intervals along the stack, as depicted in Fig. 1(5). It was expected that a staggered protrusion of rectangular plates would enhance three-dimensionality and longitudinal vorticity. Hence only a single-start helix was suggested, leaving part of the surface bare. Walshe and Wootton [15] argued that although such a means may be effective under certain circumstances, the method cannot be relied on and, at some angles of inclination of the flow, the plates may have a detrimental effect.

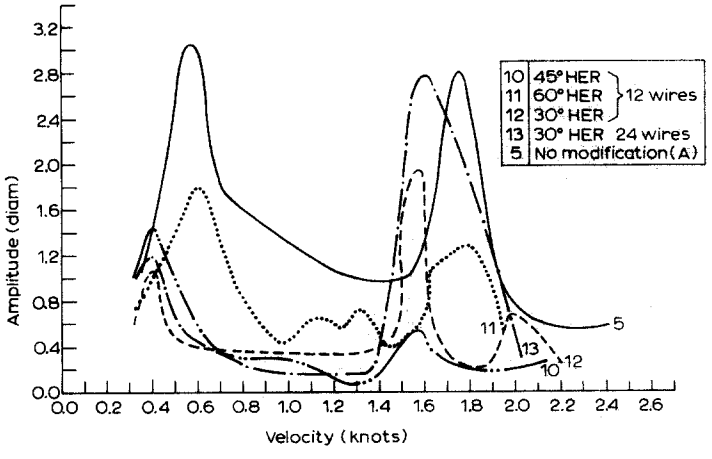

Fig. 9. Effect of helix angle on the reduction of amplitude for "herringbone" winding (after Sallet and Berezow [20]).

Sallet and Berezow's [20] "herringbone" pattern of helical winding (Fig. 1,6) disrupts the possible skewing of the flow along the cylinder by winding wires in a single direction. Tests were performed in water in the subcritical regime on a cylindrical buoy freely floating at the end of a long mooring cable having an aspect ratio of 5. Such a lightly restrained and damped system produced a maximum amplitude exceeding $3D$. Figure 9 shows the effect of various modifications of the herringbone configuration in reducing the amplitude of oscillation. The lowest amplitude was achieved with a 45° helix ($8D$ pitch), but the use of a large number of nylon ropes too small in size ($d = 0.03D$) presumably prevented better suppression of vibration.

*The original paper was not available to the present author.

3.5 Unidirectional means

In some practical applications the velocity direction does not change with time. Typical examples are horizontal pipelines, submarine periscopes, heat exchanger tubes, piles subjected to tide, etc.

Price [21] carried out tests in water on a cylinder fitted with four or eight longitudinal fins having heights of $0.2D$ and equally distributed around the circumference. He found that the configuration with four fins forming an X cross possessed only unidirectional effectiveness, the direction being as shown in Fig. 1,7. Eight fins were not effective with the stagnation point either coinciding with one fin or being half way between the fins. Alexandre [23] also claimed that the configuration in Fig. 1(7) was fully effective for unidirectional wind flow.

It might be expected than an odd number of fins would impair vortex formation and shedding, due to asymmetry. Mahrenholtz and Bardowicks [26] found that five fins fitted evenly around a stack (Fig. 1,8) considerably enhanced the amplitude of oscillation. Tests on the cylinder model with five fins in the wind tunnel in the subcritical regime also produced more intense excitation than that found for the plain cylinder. The additional excitation was particularly strong when the orientation of fins was within $-18° < \alpha < 18°$. The maximum excitation occurred for the symmetrical orientation, $\alpha = 0°$, and $V/ND = 7$. Figure 10 shows the measured drag and lift coefficients for various orientations of fins with respect to the oncoming flow. The maximum drag coefficient of 2.7 occurred when the stagnation point coincided with the

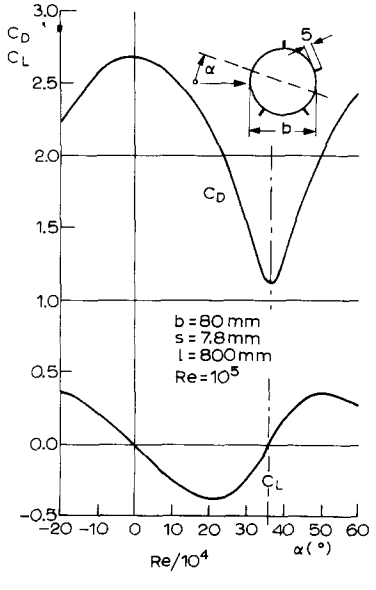

Fig. 10. Drag and lift coefficients for cylinders with five fins (after Mahrenholtz and Bardowicks [26]).

fin, i.e. $\alpha = 0°$, and the minimum of 1.1 was associated with the stagnation point being half way between two adjacent fins.

Gartshore et al. [27] fitted a cylinder with a pair of fins (having a height of $0.1D$) sidewise, as depicted in Fig. 1,9. The wind tunnel tests on a flexible two-dimensional model were carried out in smooth and turbulent flows. The amplitude of oscillation was higher for the turbulent flow throughout the tested range of reduced velocity, $4 < V/ND < 6$*. At $V/ND = 6$, the amplitude of oscillation was five times that found for the plain cylinder. Hence the attachment of side fins has a much stronger adverse effect than attachment of five fins.

Naumann et al. [22] demonstrated that the regular vortex shedding behind a stationary cylinder can be induced and maintained throughout the supercritical range by fitting "separation wires" parallel to the cylinder axis. The "separation wires" control the position of separation and straighten the separation line along the cylinder. In order to reduce and suppress regular vortex shedding the separation line should be made irregular and discontinuous, thus creating sufficiently strong three-dimensional disturbances. The advantage

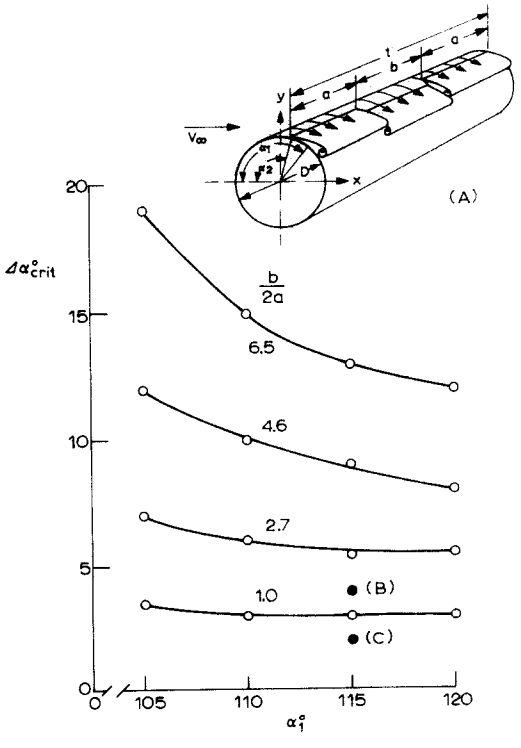

Fig. 11(A). Critical angle difference between staggered separation wires (after Naumann et al. [22]).

*The maximum amplitude has not been reached in these tests.

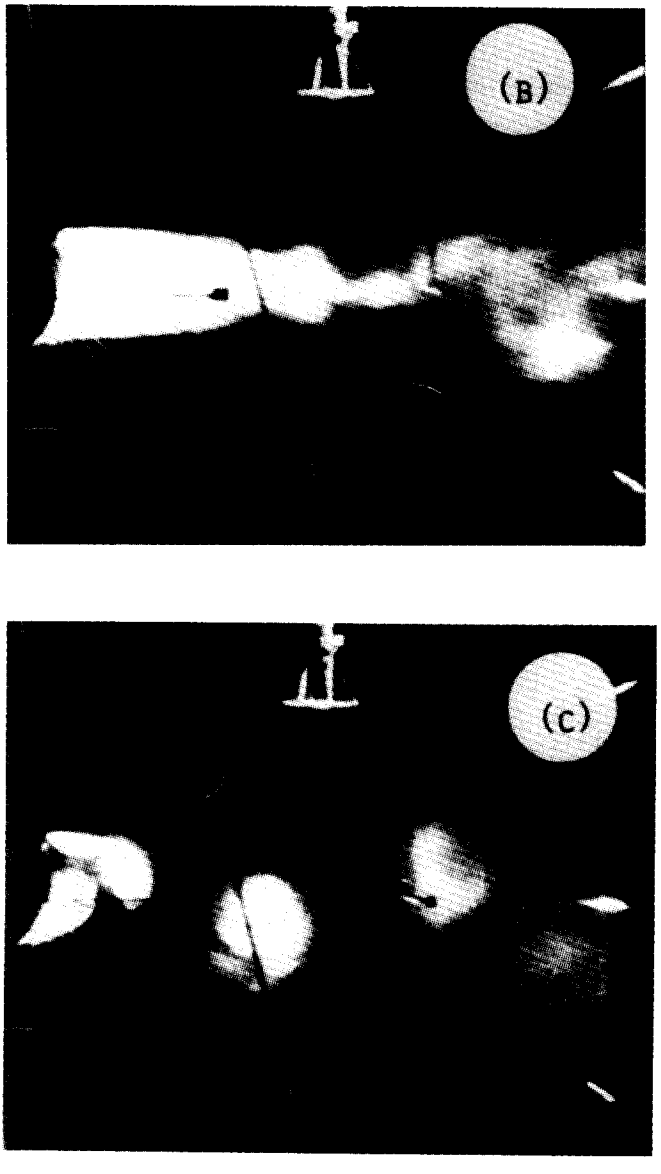

Fig. 11(B) and (C). Measurement of fluctuating velocity due to vortex shedding: refer to Fig. 11(A) (after Naumann et al. [22]).

of controlling separation at its origin in this way was that very thin wires having a diameter of only $0.013D$ were effective.

The irregularity of the separation line along the cylinder was induced by staggered separation wires as sketched in Fig. 11(A). The two separation wires, each of length a, were fixed on the surface along the cylinder at an angle α_1 measured from the stagnation point. The third separation wire, of length b,

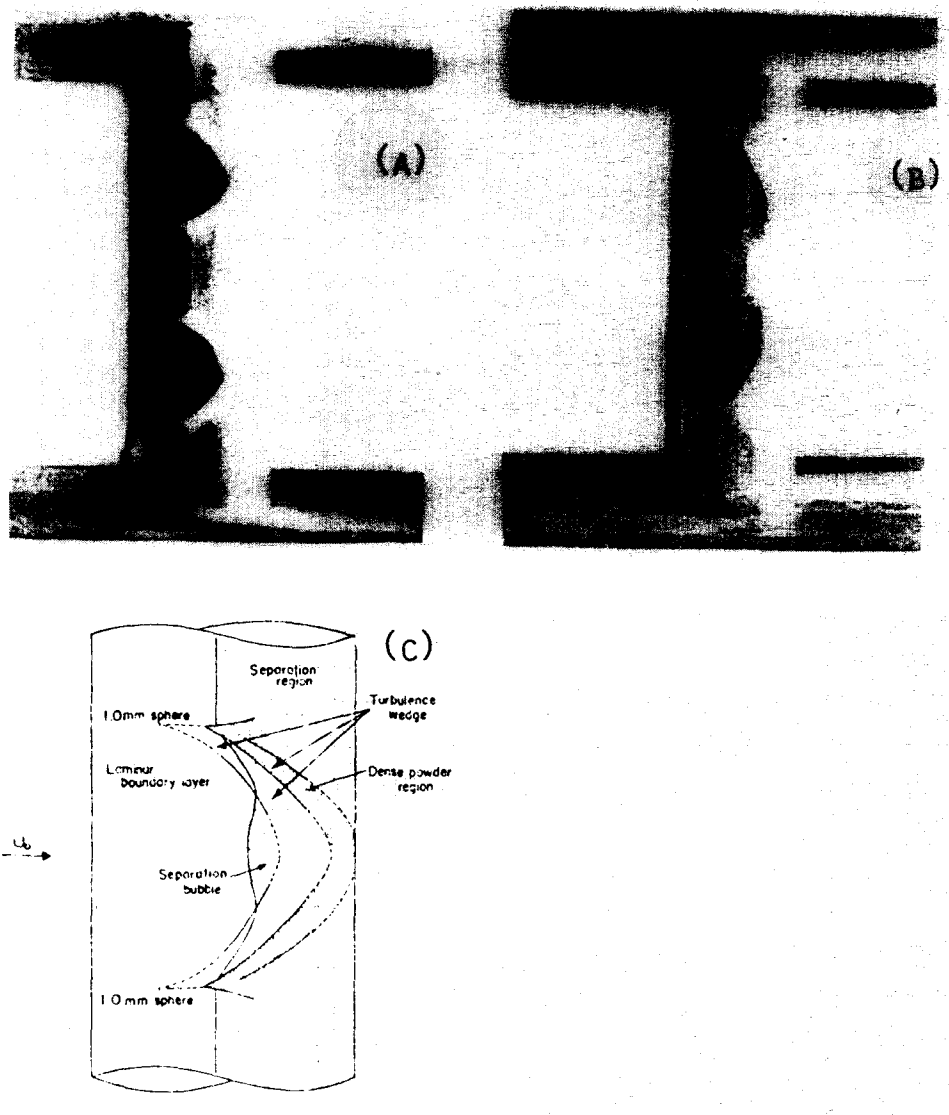

Fig. 12. Separation lines induced by small spheres: (A) Re = 1.1×10^5, (B) Re = 2.8×10^5, (C) schematic interpretation of patterns (after Mizuno [24]).

could be fitted at any angle α_2 such that $\alpha_2 > \alpha_1$. The fluctuating velocity due to vortex shedding was measured by a hot wire located near to and outside of the wake, see Fig. 11(B) and (C). The third separation wire was moved to various positions by increasing the angle α_2 until the periodicity of vortex shedding as detected by the hot wire was lost. This point marked a critical angle-difference $\Delta\alpha$, as shown in Fig. 11(A). It is evident that a stagger of only 4° is sufficient to disrupt vortex shedding when $a = b/2$. The effectiveness of the

staggered wires was decreased rapidly by increasing the length of the third separation wire and moderately improved by shifting the two fixed wires towards higher angles α_1. Figure 11(B) and (C) demonstrates convincingly the effect of staggered wires in the critical regime.

It may be argued that the effectiveness of staggered separation wires is strongest if they are applied in the critical regime (natural separation at 120°) and possibly in the postcritical regime (natural separation around 100 and 105°). The applicability of this method in the subcritical regime (natural separation at 80°) and on flexible models has not been verified. The staggered separation concept was embodied in Alexandre's [23] proposal of welded longitudinal plates (Fig. 1,11). The spread of plates around the circumference provides an omnidirectional effectiveness.

Further development of controlled separation was elaborated by Mizuno [24] who introduced surface excrescences in the form of small spheres attached to the surface (Fig. 1,12). The spheres were attached at ±60° from the stagnation point and spaced $0.6D$ apart along a short cylinder. The wake behind the spheres perturbed the transition to turbulence in the boundary layer on the surface in such a way that an irregular separation line was formed in the high subcritical range (Fig. 12(A)) and a symmetrical wavy separation line in the critical regime (Fig. 12(B)). The interpretation of the chalk-dust pattern by Mizuno is also shown in Fig. 12(C). It should be noted that the spheres became ineffective in the lower subcritical and postcritical regimes.

Mizuno did not consider that this technique could be applied as an aerodynamic means of suppressing vortex shedding and consequently he did not test its effect on a flexible cylinder (hence there is no indication + or − in Fig. 1,12). It should be mentioned, however, that the attachment of studs in staggered rows around the surface of the buoy tested by Sallet and Berezow [20] showed only modest effectiveness in reducing the amplitude of vibration.

4. Shrouds

4.1 Perforated shrouds with circular holes

Price [21] carried out an extensive study of the effect of various surface modifications on reducing oscillations of a circular cylinder submerged and towed in water. A wide variety of straight and helically wound wires and longitudinal fins was tested in the subcritical regime and found to possess only limited effectiveness. Price also tried to change the cross-sectional area of the model locally by fitting concentric bushings $1\frac{1}{4}D$ in diameter and $1.5D$ apart. The maximum amplitude of vibration of the cylinder with bushings exceeded that of the plain cylinder. Price subsequently diverted his tests to a device detached from the surface which he called a perforated shroud.

Price [21] thought that "the shroud would break up the flow into a large number of small vortices with the result of minimising the periodic asymmetry of flow about the cylinder." The shroud proved to be an effective means for all stiffnesses of the tested cylinder, as seen in Fig. 13(A) where

for comparison the envelopes of maximum amplitudes for shrouded and plain cylinders are shown as dotted curves. The relative double amplitude of oscillation is depicted on the vertical axis whilst the stiffness of the spring holding the cylinders is plotted along the horizontal axis. The log—log scale spreads the low stiffness range ($20<k<200$) with large amplitudes, and clearly shows that the shroud is least effective in that range. At higher stiffnesses (i.e. a less flexible cylinder), a steep decrease in maximum amplitude occurs and the effectiveness of the shroud is markedly improved. For example, the double amplitude (of $0.7D$) found for the plain cylinder was reduced by 97% after fitting the shroud.

An explanation for the effectiveness of the shroud was provided by Price [21] by comparing the flow pattern behind the plain and shrouded cylinders. Figure 13(B) and (C) shows that the individual vortices streaming in rows be-

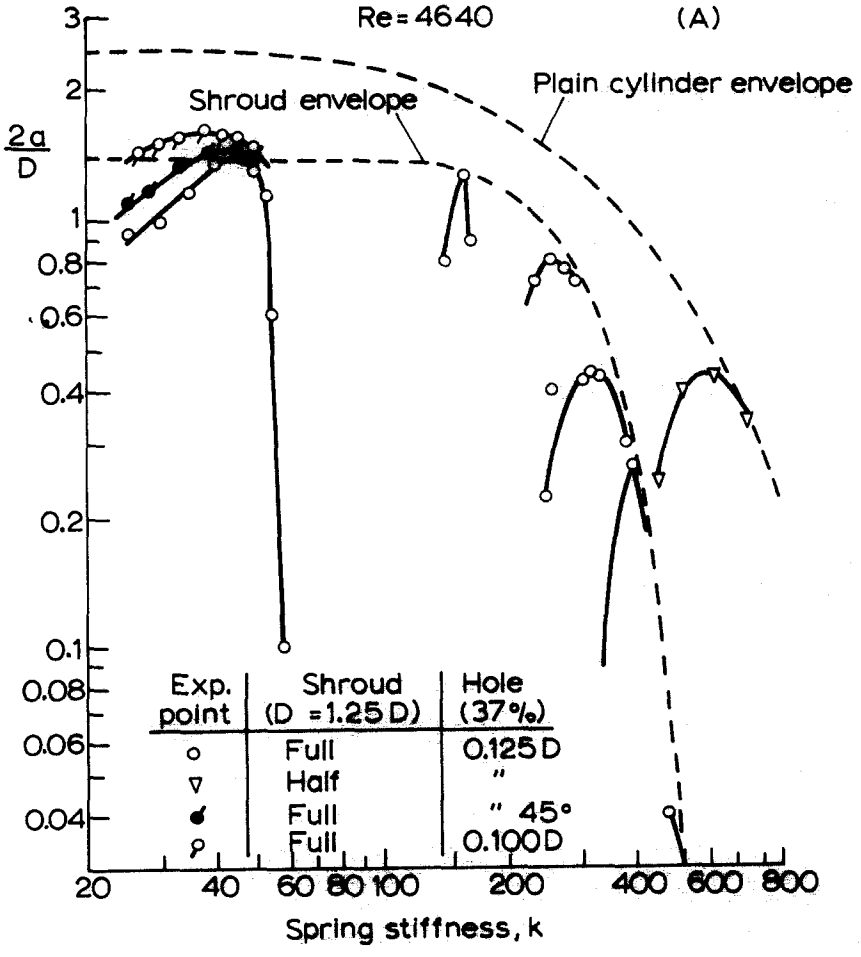

Fig. 13(A). Effectiveness of perforated shrouds (after Price [21]).

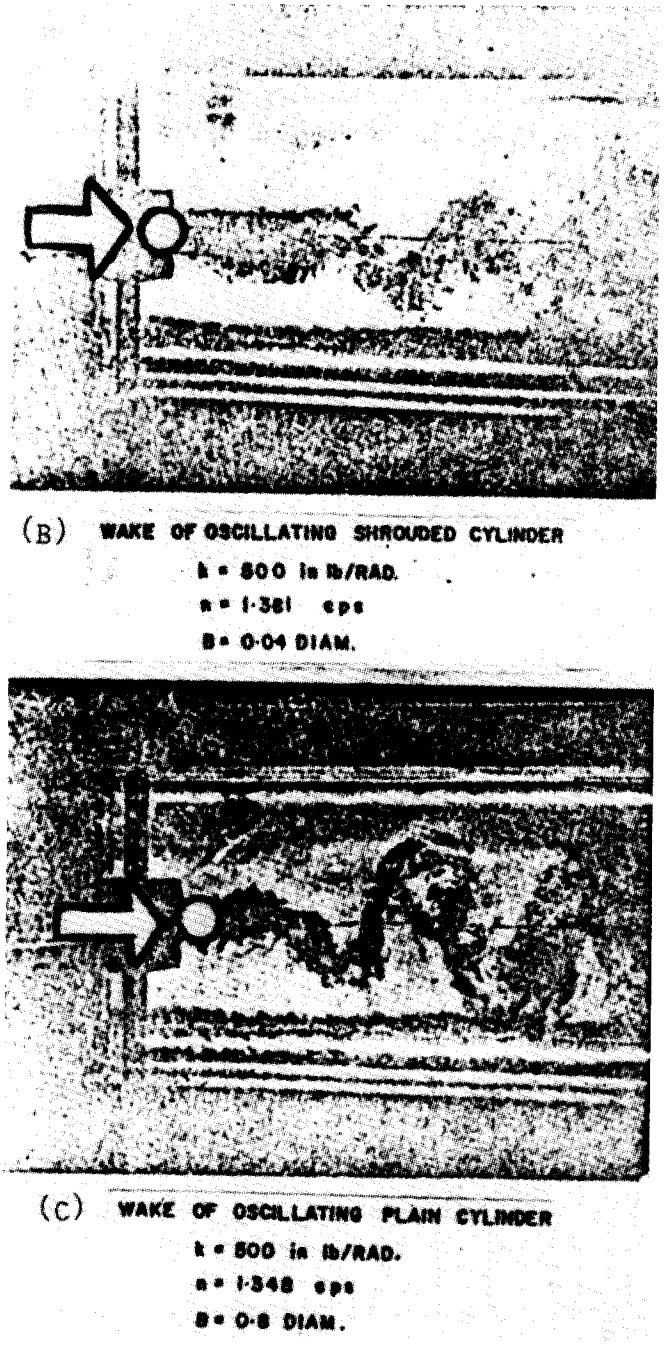

Fig. 13. (B) Wake behind shrouded cylinder, and (C) wake behind plain cylinder (after Price [21]).

hind the shrouded cylinder are smaller, more closely spaced, and form several diameters further downstream along an apparently stable nearwake, than the vortices shed behind the plain cylinder. Hence, the effect of the faraway vortices was so small that the double amplitude in Fig. 13(C) of $0.8D$ diminished to $0.04D$ in Fig. 13(B).

The perforated shroud had a diameter $1.25D$; the porosity was 37% (ratio of the area of all holes divided by the total shroud area), the hole diameter was $0.1D$ and the shroud covered the cylinder completely. The shroud became slightly more effective when the hole size was increased to $0.125D$ whilst the porosity was held constant. Rows of holes parallel and perpendicular to the axis proved more effective than rows inclined at 45°, as can be seen in Fig. 13(A). The application of the shroud to the lower half of the immersed length of the cylinder resulted in a reduction of effectiveness in the subcritical regime.

Price [21] also carried out additional tests in the wind tunnel within the range $1 \times 10^5 < \mathrm{Re} < 4.5 \times 10^5$. The critical regime for the plain cylinder occurred at $\mathrm{Re} = 2.5 \times 10^5$ with a characteristic fall of the drag coefficient to 0.3. The drag measurements on shrouded cylinders showed that the drag coefficient remained substantially constant throughout the tested range of Reynolds numbers. The drag coefficient* was 0.6, intermediate between the subcritical and supercritical values for the plain cylinder. The use of smaller holes and the increase in the gap between the shroud and the cylinder increased the drag to 0.66 and 0.72, respectively.

The low drag of the perforated shroud (which is an omnidirectional means) is a highly advantageous asset. Price rightly concluded that the constancy of the drag coefficient implies that the nature of the flow about the shrouded cylinder also remained substantially unchanged within the tested range of Reynolds numbers.

It might be interesting to mention that a perforated shroud with circular holes destabilises the wake in supersonic flow [44]. The wake shock, a typical feature found at the end of a narrow wake, disappeared behind the perforated shroud at a Mach number of 2.4.

4.2 Shrouds with square holes

Further evolution in the geometry and confirmation of the effectiveness of the perforated shroud in the postcritical regime have been made by Walshe [45]. He found that square holes are more effective than circular ones. Knell [46] measured the drag of two shrouds with square holes having porosities of 20 and 36% ($0.07D$ and $0.05D$ sizes of holes) on infinite aspect ratio and free-ended models. The Reynolds number range was $8 \times 10^4 - 3 \times 10^6$. The drag coefficient for a shrouded cylinder was ~0.9 based on the cylinder diameter, and showed very little dependence on Reynolds number, being almost indistinguishable for the two porosities. Wootton and Yates [47] extended drag measurements to separate the drag exerted on the shroud from

*The drag coefficient was based on the shroud diameter.

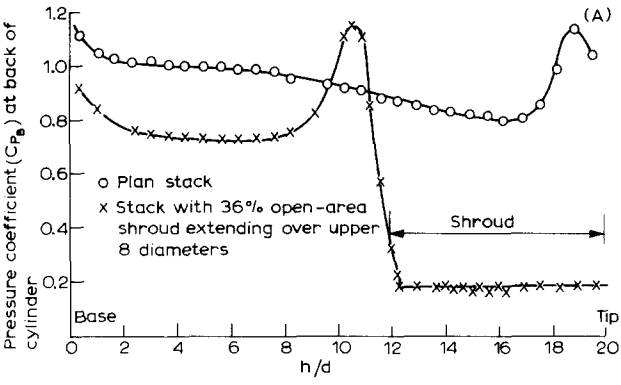

Fig. 14. (A) Pressure distribution along the downstream side of stack; (B) surface flow pattern (after Wootton and Yates [47]).

that experienced by the cylinder. They found that the drag coefficient of the shroud was 0.7 and for the enclosed cylinder 0.2 (both based on the cylinder diameter).

Figure 14(A) shows the distribution of the pressure coefficient at the back of the cylinder, the so-called "base pressure", which is proportional to drag. At $Re = 10^5$ there is a pronounced peak of local drag near the tip, which moved to just below the base of the shroud when this was fitted. The pressure distribution on the lower $12D$ was almost identical to that on an $L/D = 12$ stack without a shroud. At much higher Reynolds numbers, which were applicable to full-scale stacks, the peak loading at the tip of the stack still existed, although the overall drag levels were lower, as documented by Gould et al. [48].

The surface flow pattern on the cylinder, seen after removing the shroud, is shown in Fig. 14(B). It is evident that the separation line is much further back on the part of the cylinder beneath the shroud than on the unprotected part. Just below the shroud, a "foot" of a strong vortex can be seen (Fig. 14(B)) which is typical for the flow near the top of a plain stack [48]. The dominant pattern underneath the shroud is set by the radial lines of holes up to the separation lines.

It might be worthwhile to mention that Wootton and Yates [47] carried out some experiments with a modified shroud made up from rings connected by three longitudinal ribs. Flow patterns similar to those shown in Fig. 14(B) were obtained, but despite that, the ring shroud proved to be less effective in suppressing vortex-induced oscillations. It seems that the observed surface flow pattern is not responsible for the effectiveness of the square-holed shroud.

A brief study of the effect of the square-holed shroud on buffet amplitudes of two cylinders in a tandem arrangement was made by Walshe and Cowdrey [49]. Two flexibly mounted cylinders were placed 9 diameters apart and fitted with perforated shrouds over the top quarter of the model height. It was found that the shrouds were of limited benefit only. The rear cylinders oscillated not only because of self-generated vortex shedding but also because of the buffeting action of the eddies produced by the front cylinder. The worst oscillations of the downstream plain cylinder occurred when the upstream one was shrouded. The large-amplitude vibrations persisted when both cylinders were shrouded and some effectiveness was noticeable only when the upstream cylinder was plain and the rear shrouded.

Another interesting observation was made for the upstream cylinder. The maximum amplitude for the single plain cylinder having a damping factor $M\delta/\rho D^2 = 3.7$ was $0.13D$, but placing the shrouded second cylinder $9D$ behind it increased the maximum amplitude of vibration of the upstream one by at least 30%. These peculiar effects will be discussed in some detail in the final Section.

4.3 Fine-mesh gauze shroud

Some further understanding of the processes generated by perforated shrouds is gained by describing other shroud geometries. Most of the tests described so far did not have a reduced velocity exceeding 10 or so, at which the amplitude of oscillation of the plain cylinder subsided to a low level. Moss [50] extended his tests up to the reduced velocity of 45 and found a continuous build-up of amplitude. At the end of his test range the amplitude of oscillation of the plain cylinder was comparable with the peak amplitude found at $V/ND = 5$. Similar alarmingly large amplitudes were measured on full-scale stacks by Ozker and Smith [51] in the postcritical regime $1\times 10^6 < \mathrm{Re} < 7 \times 10^6$. These large-amplitude oscillations of cylinders far away from the synchronisation range prompted Zdravkovich and Volk [28] to examine the effectiveness of various shrouds under these new circumstances.

Figure 15 shows the effect of various shrouds on reducing the amplitude at high reduced velocities. The plain cylinder displays a steep increase in amplitude similar to that observed by Moss [50]. Three shroud geometries were tested (all having 30% porosity): circular-holed, square-holed and fine-mesh gauze (No. 100, ϕ 42 S.W.G., and hole size 0.152 mm). All three shrouds were almost equally effective in suppressing vibration.

Figure 16 shows typical pressure distributions around plain and shrouded cylinders. Circular- and square-holed shrouds produce almost identical pressure

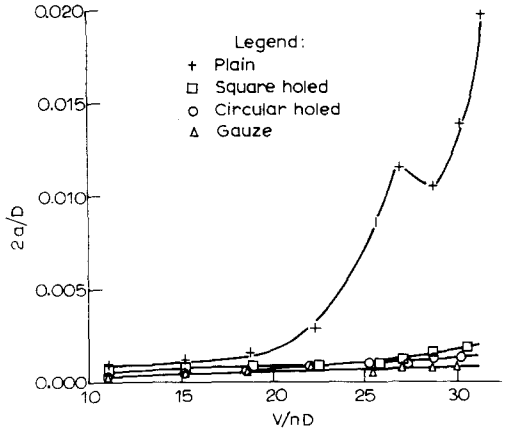

Fig. 15. Effectiveness of shrouds beyond the synchronisation range (after Zdravkovich and Volk [28]).

distributions similar to those found by Wootton and Yates [47] except that the base pressure is lower. The shroud made of fine-mesh gauze, (Fig. 1,14), which was the most effective one in Fig. 15, affected the pressure distribution around the cylinder differently than did the other perforated shrouds. A radical departure occurred between 80 and 160°, where the shrouded gauze prevented separation and forced the inner flow around the cylinder surface, with a slow rate of ejection of fluid through the gauze into the nearwake. The penalty in maintaining such a flow pattern was a higher drag coefficient, estimated to be 1.3 (Fig. 1,14).

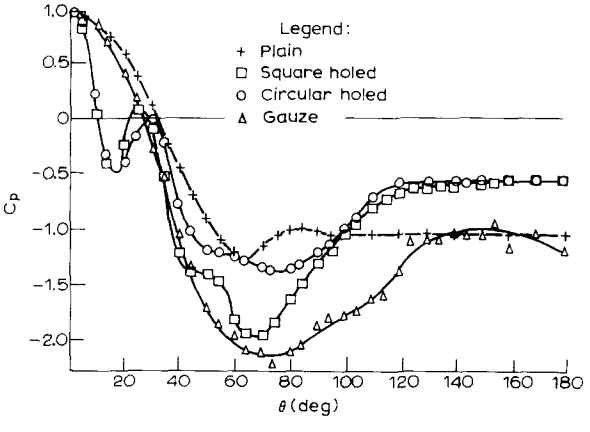

Fig. 16. Pressure coefficient distribution on shrouded cylinders, Re = 1.8×10^5 (after Zdravkovich and Volk [28]).

4.4 Axial-rod shroud

Price's [21] concept, that the shroud should break-up the flow into a large number of small vortices, has been developed further by introducing a plurality of uninterrupted bluff members parallel to the axis of the cylinder. It was expected that each bluff member should generate a vortex street of its own, which would interact with the neighbouring ones in a highly irregular manner. Zdravkovich [52] demonstrated that the interaction of three circular cylinders produced weak and fastly decaying vortex streets which soon broke down, and a new, strong, regular vortex street was formed far downstream from the remnants of the original ones. Hence it was worthwhile attempting to suppress the formation of strong vortices behind a big cylinder by enclosing it within a cluster of small cylinders, which, by generating their own tiny vortex streets, perturb the separated shear layers to such an extent that it will be several diameters downstream before a proper formation process can start.

The axial-rod shroud [29] (Fig. 1,15) was made of cylindrical rods* held in ring-spacers fixed around the cylinders, with the axes of the rods parallel to the axis of the cylinder. The ring-spacers were made of two identical halves for easy fitting to the cylinder, and by pulling out some rods (every second, third, fourth, etc.) it was possible to vary the porosity of the shroud evenly around the circumference. Figure 17(A) shows a typical axial-rod shroud fitted on the model for wind tunnel tests. The use of rods instead of perforations may prove advantageous in some applications, e.g. to avoid blocking of holes by ice formation or clogging of holes by algae in the marine environment. Several parameters were varied during the tests in order to find an optimum configuration:

(i) the porosity was varied from 24% to 96% by changing the number of rods from 218 to 4;

(ii) the shroud size, Ds/D, was varied to take the values 1.08, 1.165, 1.25 and 1.50;

(iii) the circumferential distribution of porosity was varied, leaving some portions of the circumference plain, by withdrawing rods.

Variation of the porosity had an opposite effect on shrouds of different sizes. For the $Ds/D = 1.08$ shroud, low porosities (24 and 62%) corresponded to inefficient shrouds, while high porosities (81 and 91%) led to some improvement. The most effective shroud appeared to be that with a porosity of 90%, achieved with only five rods around the cylinder at $\pm 55°$, $\pm 117°$ and $180°$. This arrangement was found to be highly effective in suppressing severe fluid elastic vibrations in tube banks [53]. It was essential that the rods or wires were always detached from the cylinder surface, in order to generate adequate vortex streets behind them; otherwise, their vortex streets were suppressed [54].

An entirely opposite trend was found for the axial-rod shroud having $Ds/D = 1.5$. The least effective shrouds were those having 62, 81 and 90% porosity.

* "Rods or tubes of circular cross-section or other suitable cross-section, oval, elliptical or other convenient shape", as stated in Zdravkovich's Patent Application.

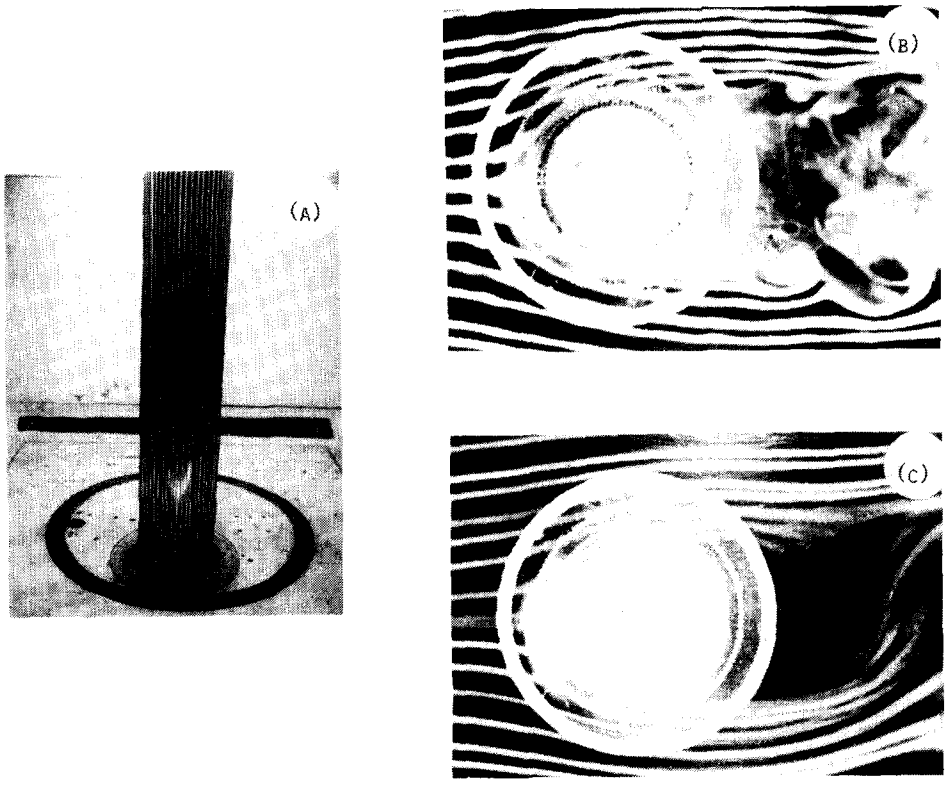

Fig. 17. (A) Axial-rod shroud in the wind tunnel; (B) nearwake behind plain cylinder, Re = 4.3×10^3; (C) nearwake behind shrouded cylinder, Re = 4.3×10^3 (after Zdravkovich [29]).

The only effective one had 24% porosity, but it was less effective than the $Ds/D = 1.08$ shroud with five rods.

The intermediate shrouds having $Ds/D = 1.16$ and 1.25 were similar in that decrease in their porosity led to an increase in effectiveness. The most effective were $Ds/D = 1.25$ with 24 and 63% porosity and, close to them, $Ds/D = 1.16$ with 62 and 81% porosity. The higher porosity of the axial-rod shroud in these cases resulted in a drag coefficient of 0.9 despite the bluff shape of the shroud members. The effectiveness was verified in water around the synchronisation range within $4 \times 10^3 < \mathrm{Re} < 1.5 \times 10^4$, and at $\mathrm{Re} = 2 \times 10^5$ in a wind tunnel.

Flow visualisation tests were carried out only at low Reynolds numbers in a smoke wind tunnel. Figure 17(B) shows the nearwake stabilisation produced by the shrouded cylinder ($Ds/D = 1.25$, 24% porosity) and contrasts this with the nearwake of the plain cylinder (Fig. 17(C)). Note the high entrainment of smoke into the nearwake from the rear of the shroud and the absence of smoke in the nearwake for the plain cylinder.

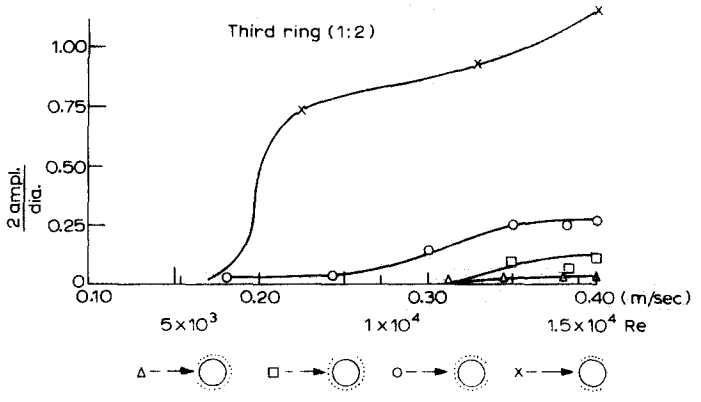

Fig. 18. Effectiveness of incomplete axial-rod shrouds (after Zdravkovich [29]).

The most effective shroud geometry (Ds/D = 1.25, 63% porosity) was chosen to examine the effect of an "incomplete" shroud. The shroud originally consisted of 52 rods but 13 rods were pulled out so that 90° of the cylinder circumference appeared unshrouded and exposed to the flow. Figure 18 shows the effect of the orientation of the unshrouded portion in relation to the free stream on the effectiveness of the incomplete shroud in reducing the amplitude of oscillation. When the unshrouded portion faced the free stream and also when it was positioned sideways the effectiveness was not appreciably reduced; when the unshrouded portion faced the nearwake the effectiveness of the shroud was reduced substantially.

An unexpectedly severe oscillation occurred with only 11 rods left on each side of the shroud, as shown in Fig.1(16). The amplitude of oscillation exceeds that found for the plain cylinder and increases throughout the tested range, as can be seen from Fig. 18. Such adverse behaviour is possibly associated with a change of the flow pattern from an intense flow between the shroud and cylinder to a sudden switch of flow around the shroud. The incomplete shroud is then analogous to two side-fins (Fig. 1,9) as described and documented by Gartshore et al. [27].

Some distortion of the shroud in high wind may be expected, which will lead to an eccentric position relative to the cylinder. The effect of axial-rod shroud eccentricity on its effectiveness was examined by Zdravkovich and Southworth [55]. Eccentricity of such shrouds in any direction improved their effectiveness in comparison with the concentric configuration. Eccentricity transverse to the flow direction caused a sharp rise in the drag coefficient.

The axial-rod shroud was found equally effective in suppressing the oscillation of two circular cylinders in a tandem arrangement [56]. The observed, large-amplitude, low-frequency oscillation of the rear cylinder when placed a short distance behind the upstream one is not caused by vortex shedding in this case. A new mechanism is responsible, in the form of flow-switching, from

flow passing through the gap between the cylinders to flow around the tandem. When both cylinders were shrouded this mode of oscillation was powerfully suppressed, both in wind tunnel and water channel tests.

4.5 Axial-slat shroud

Another variation on the theme of "plurality of axial members" was developed by Wong [31]. The members took the form of a number of slats placed longitudinally around the periphery of the cylinder (Fig. 1,18). The optimum configuration consisted of 25 slats, $0.087D$ wide, producing a "porosity" of the shroud of 40%. The shroud diameter was $1.286D$ and the drag measured within the range $1.5 \times 10^4 < \mathrm{Re} < 1.5 \times 10^5$ was almost constant at $C_D = 1.1$. The effectiveness of the shroud was attributed to control of the boundary layer separation on the cylinder and shroud. Wong [57] argued that inner flow between the slats and the cylinder was formed around the stagnation region, where the pressure was high enough to impel the fluid between the slats. The continuous ejection of fluid through the slots around the sides and through the rear was a significant factor in stabilising the nearwake and the flow around the shroud itself.

The existence of fast flow along the inner passage was confirmed by the low pressure measured along the sides of the cylinder, but only when some of the front slats had been removed, as seen in Fig. 19. The removal of some slats on the rear side facilitated the ejection of the inner flow into the nearwake. Better guiding of the inner flow can be achieved with continuous guiding-vanes as proposed by Grimminger [34], which will be described in the next Section.

The effectiveness of the axial-slat shroud for various front and rear openings is shown in Fig. 20. The point corresponding to $\theta = 5°$ corresponds to a fully slatted shroud. Only in that case was the shroud omnidirectional,

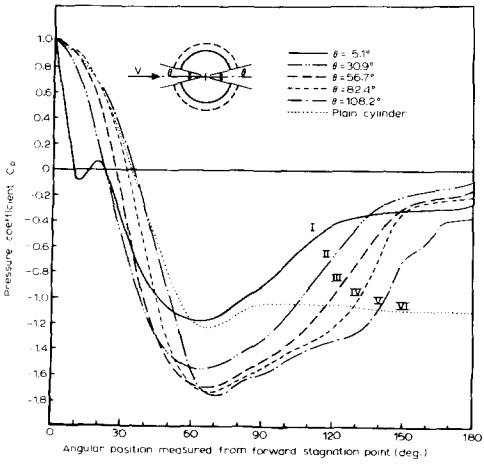

Fig. 19. Pressure distribution around fully and partially shrouded cylinders, Re = 1.2×10^5 (after Wong [57]).

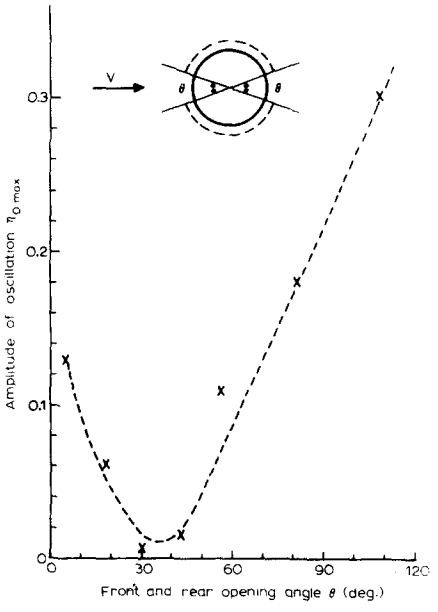

Fig. 20. The effectiveness of an axial-slat shroud for various upstream and downstream openings; 2/3 coverage, Re = 2.35 × 10^4, and $2M\delta/\rho D^2$ = 1.8 (after Wong [57]).

being unidirectional in the other cases. Figure 20 demonstrates that a significant improvement in effectiveness can be achieved by an axial-slat shroud with front and rear openings up to ±20°. Further removal of slats has an increasingly detrimental effect. The incomplete axial-slat shroud has been successfully applied in the marine environment, as reported by King [58].

The axial-slat shroud was found to be less effective in suppressing buffeting oscillation when two cylinders were in a tandem arrangement [57]. The shrouded cylinder oscillated vigorously, particularly when the spacing between the cylinders was greater than 4D. The effectiveness of the incomplete axial-slat shroud also seriously deteriorated when the openings were not aligned with the direction of flow. When the openings were positioned sidewise, the amplitude increased 40 times in comparison with that in the aligned configuration [57].

5. Nearwake stabilisers

5.1 Splitter plates

One of the earliest reported attempts to stabilise the nearwake behind bluff bodies by introducing some kind of "afterbody" is cited by Hoerner [59]. Apparently at DVL* in 1934 a triangular cylinder was attached to the rear of

*Deutsche Versuchsanstalt für Luftwissenschaft was the German Air Research Establishment.

the circular cylinder, with its wedge pointing downstream. The effect was that the drag coefficient, which was 1.19 for the plain cylinder, was reduced to 0.89. Hoerner correctly stated that the reduction of the drag was not due to a streamlining effect.

Roshko [60] carried out the first systematic tests with long and short splitter plates, attached or detached, behind the circular cylinder. The short splitter plate had a chord of $1.14D$. When it was attached to the rear of the cylinder it did not suppress vortex shedding, as can be seen from Fig. 21, though it did reduce the Strouhal number. When the splitter plate was moved downstream, leaving a gap between it and the cylinder (Fig. 1,20), the base pressure increased and the Strouhal number further decreased (Fig. 21). The Strouhal number became a minimum, and the base pressure a maximum, when the trailing edge of the splitter plate was $3.85D$ downstream of the cylinder base. What was remarkable was the abrupt jump that occurred at this position when both St and C_{pb} almost reached their original values. Roshko correctly concluded that the splitter plate delayed the formation of vortices by extending the separated shear layers downstream of its trailing edge.

Roshko [60] also tested a long splitter plate having a chord of $5D$. Figure 22 shows the pressure distribution along the nearwake with and without the long splitter plate. The minimum peak pressure behind the plain cylinder indicates the centre of the vortex formation region, and the rounded minimum half-way along the splitter plate indicates the centre of an elongated stationary eddy (as demonstrated by Bearman [61] on a different blunt body). Roshko [62] could not detect significant periodicity using a hot wire placed one or two diameters behind the cylinder and above the long splitter plate at Re = 7.5×10^3. Hence Roshko concluded that the long splitter plate was fully effective in stopping the periodic shedding. He also suggested that an even

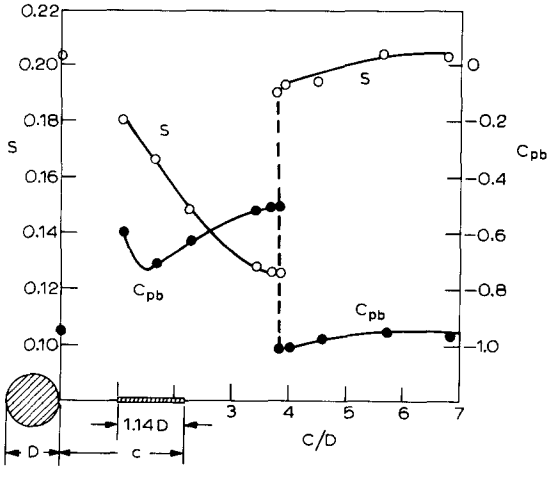

Fig. 21. Wake interference with short splitter plate, Re = 1.45×10^4 (after Roshko [61]).

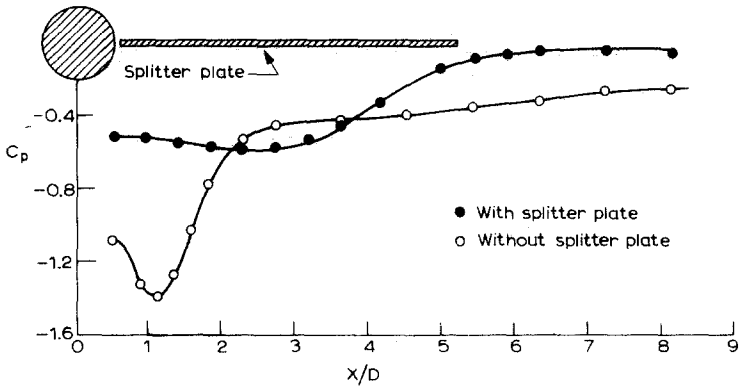

Fig. 22. Pressure along the wake axis with and without long splitter plate, Re = 1.45 x 10^4 (after Roshko [60]).

shorter length of splitter plate would be effective in destabilising the periodic shedding and that there might be a most effective design shape.

Baird [32] designed and successfully applied an aerodynamic means based on the splitter plate concept to prevent pipe-line suspension-bridge oscillation. Triangular splitter plates forming a double saw-tooth pattern were attached to the pipeline suspension bridge spanning the Colorado river near Blythe, California. The triangular splitter plates attached to the pipe were 1.5*D* deep downstream or upstream and 12*D* long along the pipe. The splitter plates on the upstream and downstream side were staggered and the combined pitch was 24*D*. It should be pointed out that the wind occurred from both sides along the river and that required a double saw-tooth pattern.

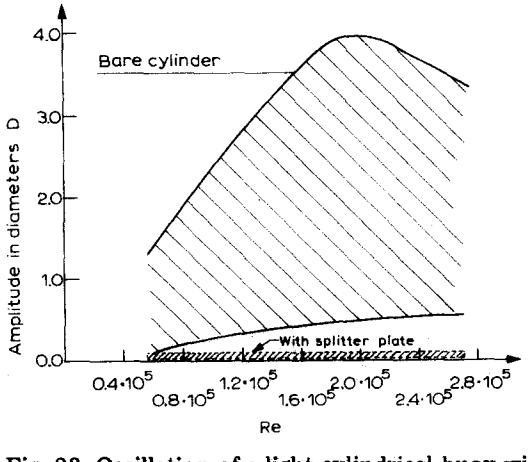

Fig. 23. Oscillation of a light cylindrical buoy with and without splitter plate, H/D = 5.15 (after Sallet [65]).

Parker [63] found that plates with bluff trailing edges may induce a powerful resonance between the vortex shedding and an acoustic wave pattern in the wind tunnel. At the resonance condition, the vortices shed were not only stronger but were also correlated over the whole span, so that the oscillating lift became very large. This in turn provided a strong acoustic source which excited the standing-wave pattern in the wind tunnel.

Gaster [64] tested a long splitter plate fitted on the upstream side of the cylinder. The splitter plate was $12.7D$ long and $0.2D$ thick and it did not affect the vortex shedding and its frequency. The only exception was within a range of velocities where a strong acoustic standing wave was generated. The frequency of vortex shedding did not change with velocity then and the hot-wire signal increased in amplitude and became very regular.

Sallet [65] applied a splitter plate as a hydrodynamic means. A low-aspect-ratio cylindrical buoy ($L/D = 5.15$) was towed in a water tank at the end of a long cable. The splitter plate was fully effective in reducing the amplitude of vibration when its length was $3D$, as seen in Fig. 23. Sallet [66] pointed out that a $2D$-long splitter plate was not effective. When the Reynolds number was in the critical regime, a splitter plate having a chord of $1.5D$ was effective in suppressing vortex-induced vibrations.

The effect of splitter plate length on the flow pattern around a stationary cylinder was investigated by Appelt et al. [67] in a water tunnel in the subcritical regime. The main findings may be grouped for short and long splitter plates as follows:

(i) *Short splitter plates* attached to the circular cylinder significantly modified the flow around them. The drag coefficient was reduced below the plain cylinder value even by a very short splitter plate and it was reduced by as much as 31% for $L/D = 1$. The vortex shedding frequency varied with L/D by $\pm 10\%$ over the range $0 < L/D \leqslant 2$. The vortex formation took place near the trailing edge of the splitter plate.

(ii) *Long splitter plates* ($L/D > 2$) progressively modified the drag and vortex shedding until $L/D = 5$. For $L/D > 5$ there was no further change; the drag coefficient was constant at 0.8 and vortex shedding behind the cylinder was eliminated, but a vortex street formed about $17D$ downstream from the cylinder fitted with a very long splitter plate. With very long splitter plates ($L/D > 5$) the flow re-attached to the plate surface at approximately $5D$ downstream from the cylinder, regardless of the splitter plate length.

Gartshore et al. [27] fitted an elastic cylinder with short splitter fins on the upstream and downstream sides. The height of the fins corresponded to a short splitter plate of $0.2D$. Two types of fins were tested; with straight and with saw-toothed edges. The pitch of the saw-toothed pattern was only $0.82D$. The vibrational responses of both finned models differed only slightly and the amplitudes were 60% of the maximum amplitude measured on the plain model. Hence short splitter plates were ineffective, despite the drastic drop in drag coefficient.

5.2 Guiding vanes

Grimminger [34] tried to stabilise the nearwake behind a circular cylinder by placing guiding vanes along its boundary. The original version of the guiding vanes consisted of two flat plates (being ~1D long) fitted along the side of the cylinder and parallel to each other and the cylinder axis (Fig. 1,21). The essential feature of these guiding plates was that they were fixed away from the cylinder by screws and washers placed 2.5D apart; the gap between the guiding plates and the cylinder surface was 0.1D. Hence the guiding vanes did not interfere with the boundary layers and the "communication" between the separated shear layers was not affected. The guiding plates reduced the drag coefficient from 1.06 measured on the plain cylinder* to 0.83, and oscillations caused by the vortex street were successfully reduced to a low amplitude. It should be pointed out that a splitter plate of the same length reduced the drag to C_D = 0.95 but did not appear to be effective in suppressing oscillations.

Grimminger [34] also improved his hydrodynamic means by replacing the plates with vanes, as depicted in Fig. 1(22). The additional set of bolts and double nuts at the end of these curved guiding vanes, which were necessary to hold them stationary, did not affect a further reduction of the drag coefficient to 0.65. Final improvement was achieved by extending the leading edges of the guiding vanes around the cylinder upstream up to around ±45°. The overall streamlining was so improved that the drag coefficient was reduced to 0.51. Thus it appeared that the oldest hydrodynamic means invented in 1945 had the lowest drag coefficient of all those shown in Fig. 1.

Wood [68] carried out experiments on mechanically forced lateral vibrations of a blunt aerofoil having a base in the form of a square-section cavity. The

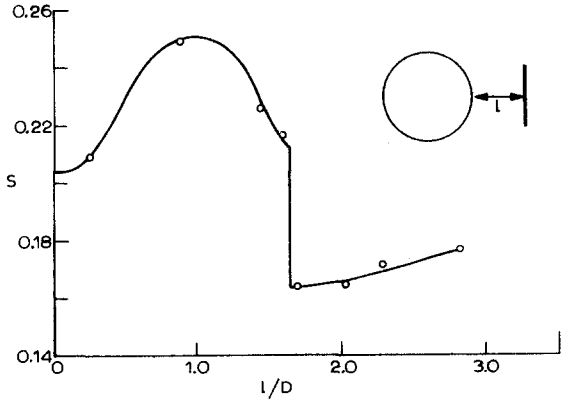

Fig. 24. Strouhal number variation with vertical plate distance (after Gerrard [69]).

*The model was towed in water at Re = 1.7 × 10^4 and the aspect ratio was 24, but the endplate was fixed on one side only.

model was similar to Grimminger's original concept shown in Fig. 1(21) except that the model was not a circular cylinder and that there was no gap between the cavity plates and the aerofoil. Flow visualisation revealed that there was distinct vortex shedding behind the stationary model and that the cavity itself did not stabilise the nearwake. When the model was set in heaving motion the vortices were trapped inside the cavity and the vortex street was almost completely destroyed.

Gerrard [69] made an unexpected discovery that "guiding" of the nearwake may be achieved with a flat plate positioned perpendicularly in it. He measured only the vortex shedding frequency and found a distinct fall as seen in Fig. 24. It is not known how these changes would affect the response of an elastic cylinder fitted with such a plate. Gerrard noticed that the formation region expanded to include the plate when it was close to the body, and consequently the fluctuating lift on the cylinder was expected to diminish.

5.3 Base-bleed

Wood [35] studied the effect of "base-bleed"* on an aerofoil section with a blunt trailing edge. The model, resembling an inverted letter D, had a length-to-height ratio of 10. A uniform base-bleed velocity over the middle 80% of

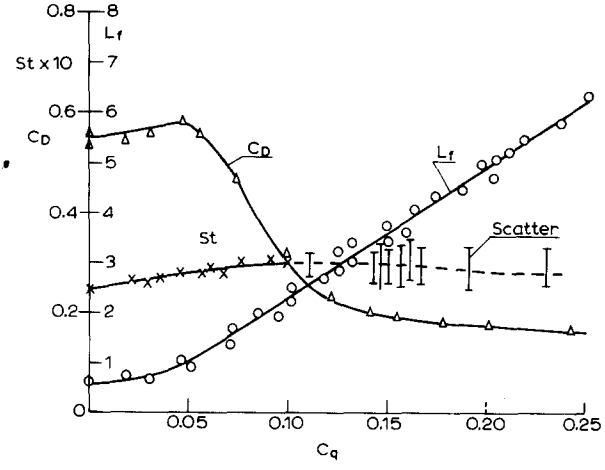

Fig. 25. Strouhal number, drag coefficient and length of formation region for various rates of base-bleed (after Wood [35]).

the span was achieved by careful adjustment of the internal configuration. The bleed coefficient was defined as the ratio of the bleed flow rate per unit span divided by the free stream flow rate through the model height per unit span. Figure 25 shows the effect of the base-bleed on the drag coefficient, Strouhal number and, most important of all, on the position of the vortex

*The actual flow rate of the fluid ejected at the base was so low that the process was called "base-bleed".

formation region. It is evident that base-bleed reduced drag by delaying the formation region further downstream. The optimum base-bleed rate was suggested to be $C_q = 0.125$.

Wood [70] also carried out flow visualisation in water in order to investigate the modifying effect of base-bleed. The results suggested that the observed decay in the vortex structure of the wake was related to variations in the conditions of mixing between the base fluid and the external stream. A remarkably clear photograph of the nearwake modifications as affected by the in-

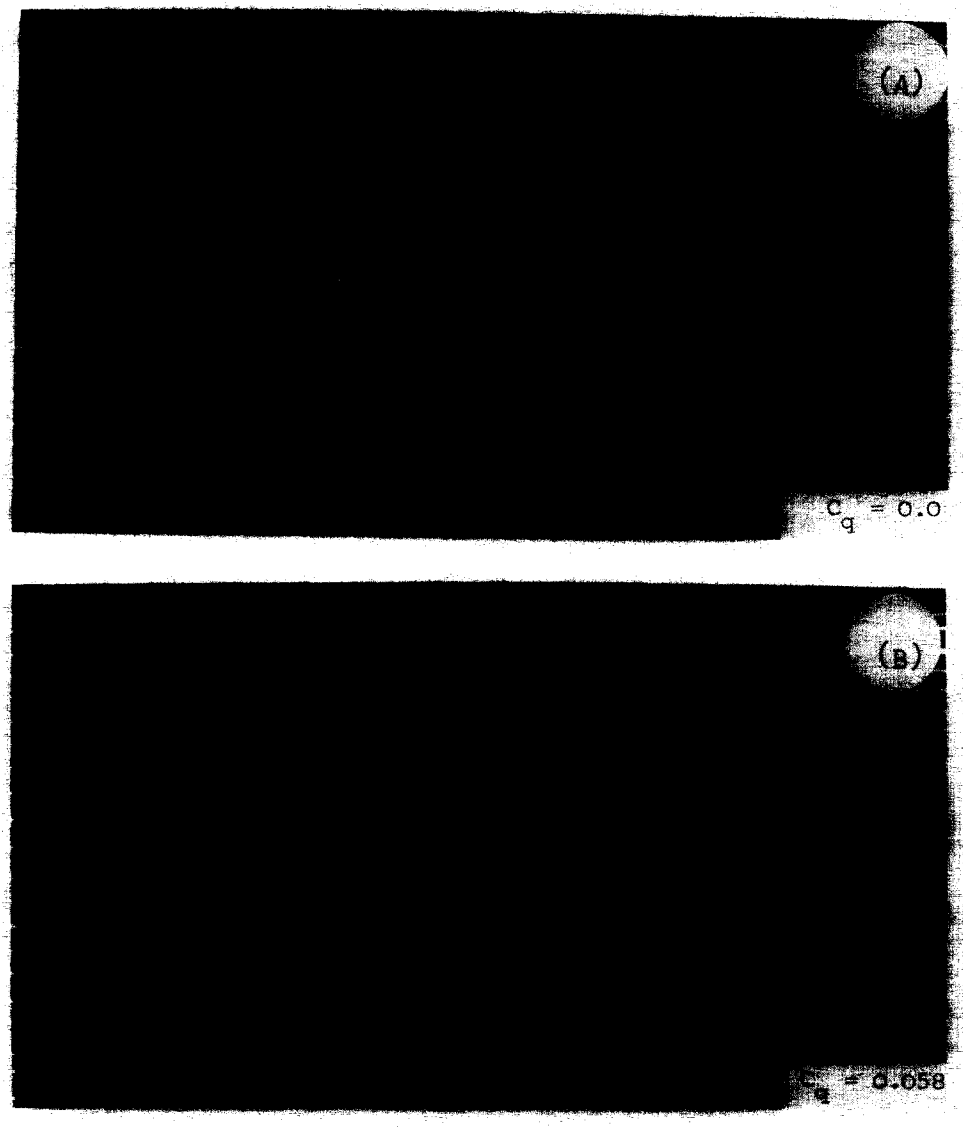

Fig. 26. Smoke tunnel model with base-bleed at Re = 1.72×10^3 (by courtesy of Dr. P.W. Bearman (unpublished)). (A) $C_q = 0.0$; (B) $C_q = 0.058$.

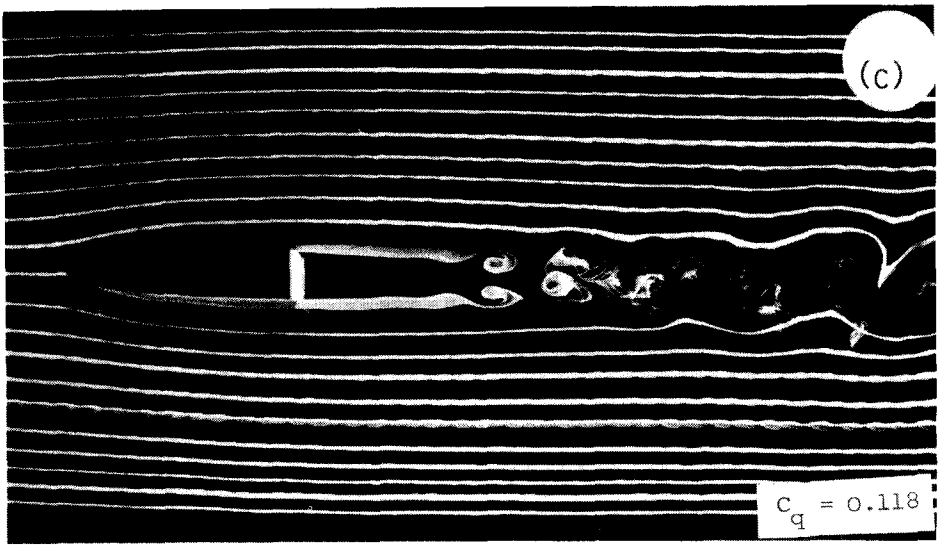

Fig. 26 (*continued*). (C) C_q = 0.118 (see Fig. 26(A)) (by courtesy of Dr. P.W. Bearman (unpublished)).

creasing rate of base-bleed is shown in Fig. 26*. The vortex formation region occurred behind the blunt base of the half-elliptic model without base-bleed, $C_q = 0$. At a low base-bleed rate, $C_q = 0.058$, the vortex formation region was displaced downstream. The nearwake appeared so stabilised at $C_q = 0.118$ that formation of a symmetrical vortex street was possible at first.

Wood [35,68,70] and Bearman did not extend their tests to circular cylinders. The reason was that a pumping system cannot be expected to be a viable alternative to simple geometric means. Igarashi [36] overcame this objection by providing his circular cylinder with a slit cut along the whole span (Fig. 1,24). Thus self-injection of fluid into the nearwake was achieved by high pressure around the stagnation region and low pressure around the base. Igarashi measured the drag coefficient and Strouhal number for two widths of the slit, 0.08D and 0.185D, at Re = 4.5×10^4. The drag coefficients were 0.9 and 0.75 and the Strouhal numbers 0.26 and 0.32, respectively. The flow pattern behind the cylinder with a 0.08D slit had a downstream displacement of the vortex formation region similar to that shown in Fig. 26.

Igarashi varied the self-injection rate by rotating the cylinder with the slit so that the slit axis became inclined to the free stream velocity up to 30°. The drag coefficient was calculated from the pressure distribution, and the flow rate through the slit was measured by a traversing hot wire. Figure 27 shows that the 0.08D slit was not wide enough to provide an optimum flow rate into the nearwake whilst the 0.185D slit was too wide. Nitoh's unpublished

* These unpublished photographs were taken by Dr. P.W. Bearman at Cambridge in 1964.

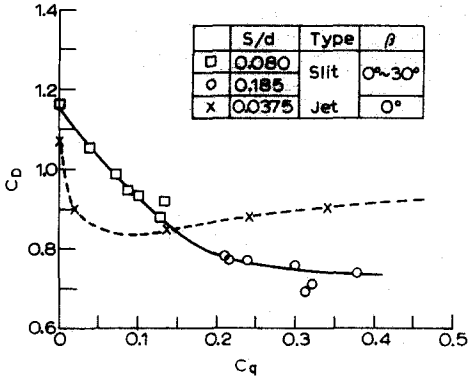

Fig. 27. Effect of slit and jet on drag coefficient (after Igarashi [36] and Nitoh (unpublished M.Sc. thesis)).

results* on drag coefficient reduction by base-bleed are also included in Fig. 27 for comparison. The effect of the slit on oscillation of an elastic cylinder was not dealt with by Igarashi [36].

6. Comparative assessment of effectiveness

The review of various means for suppressing vortex shedding from a cylinder reveals that the effectiveness depends not only on the Reynolds number, structural damping, regime of flow and the geometry of the means, but also on the displacement of the cylinder itself. The governing factor for high effectiveness is the distance of the formation region from the cylinder. The better the means, the further the displacement of the formation region downstream. It is remarkable that even the best means, such as a long flat plate, do not inhibit vortex shedding altogether but postpone it to occur as far downstream as $17D$. Hence the vortex shedding mechanism appears indestructible: it can be delayed and weakened but never totally destroyed**.

Oscillation of a plain cylinder always leads to a shortening of the nearwake and brings the formation region closer behind the cylinder. The same tendency exists when the various means are attached to the cylinder. The oscillations affect the effectiveness of the means in direct proportion to their amplitude. The means that are highly effective for low-amplitude oscillation, such as the perforated shroud, reduce large amplitudes of oscillation only to a modest 50%, as evident from Fig. 13. Unidirectional means, such as the splitter plate or guiding vanes, are the only ones capable of preventing the adverse return of the

*T. Nitoh, M.Sc.Thesis, University of Tokyo, 1971 (in Japanese).

**Taneda [71] found that the normal vortex street disintegrated downstream, but that farther downstream a new vortex street formed on a bigger scale. This process repeated itself several times up to $800D$ downstream.

formation region nearer to the cylinder. Hence, it appears that at present there is no omnidirectional means effective for very lightly damped structures. The influence of displacement is such that the only sure way of proving effectiveness is to test dynamic models.

The peculiar reduction of effectiveness due to proximity of other structures may be explained by interference with the length of the formation region. The downstream cylinders in the in-line arrangement tested by Vickery and Watkins [42] affected the position of the formation region and rendered the helical strakes ineffective. It was found, however, that when the flow was at 28° to the in-line configuration the means were effective despite the fact that this orientation gave the worst case for the plain cylinders. Similar displacement of the formation region upstream occurred when the second cylinder was placed 9*D* downstream in Walshe and Cowdrey's tests [49].

Few comparative tests have been done to evaluate various means on the same model under identical test conditions. Borges [72] carried out such an experiment on a model of a UHF television aerial. The cylindrical surface had circumferential rings, as shown in Fig. 28, and the aspect ratio was 11. The vibrational responses of the "plain" model and of that fitted either with helical strakes (Fig. 1,1) or longitudinal plates (Fig. 1,11) are shown in Fig. 28 at $2 \times 10^4 < \mathrm{Re} < 2 \times 10^5$. The helical strakes appeared more efficient than the rectangular plates, and produced 9% lower drag coefficient than the latter.

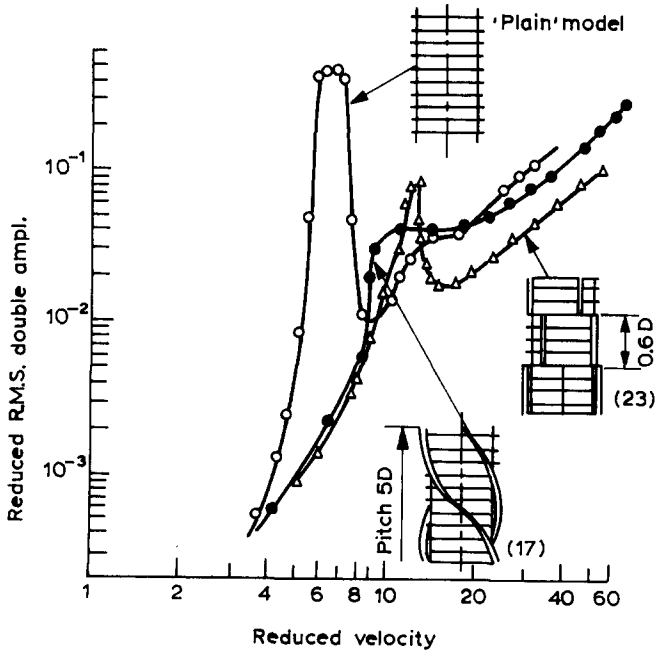

Fig. 28. Comparison of effectiveness of helical strakes and longitudinal fins (after Borges [72]).

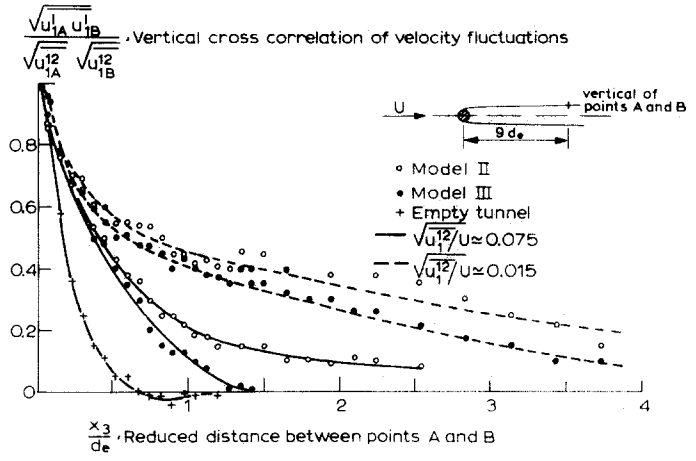

Fig. 29. Cross-correlation curves of longitudinal velocity fluctuations (after Borges [72]).

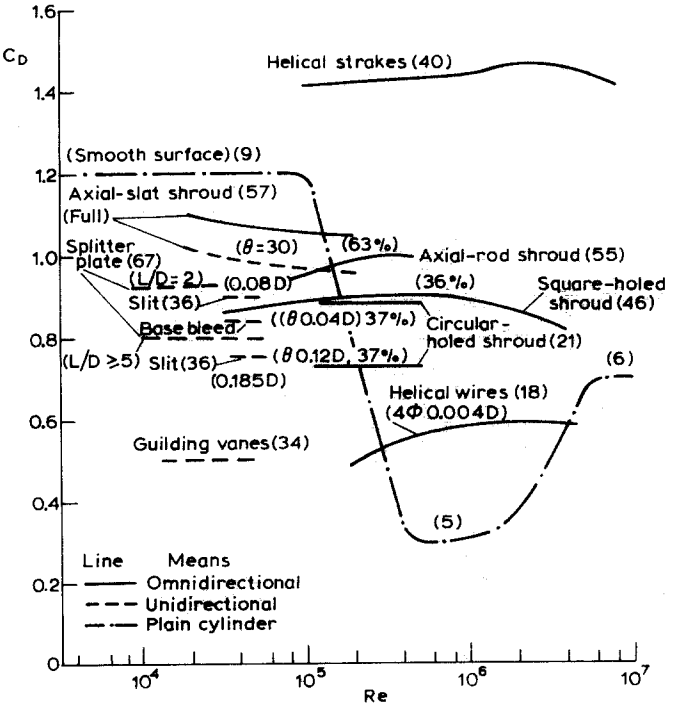

Fig. 30. Drag coefficients for various means.

The effectiveness in the post-synchronisation range changed in favour of the longitudinal plates, although an unabated rising trend was evident for both means (see Fig. 28).

The quantification of effectiveness can be expressed in terms of either the amount of structural damping required to limit the response amplitude of oscillation to prescribed values [45] or vice versa. The former has a practical appeal and the latter is more convenient from the experimental stand-point. Tests are needed for reliable quantitative assessment in all three flow regimes. The percentage reduction of amplitude, which has been adopted as a criterion by many authors, depends very much on structural damping, length-to-diameter ratio, free stream turbulence, surface roughness, etc., and hence cannot be used for comparison. Thus comparative tests of various means under identical test conditions are necessary even for apparently "equally" effective means. A research programme of this kind is currently in progress at Salford.

Another neglected area of research was and still is the measurement of the correlation of velocity fluctuations along the span of the cylinder. Borges [72] provided data for his aerial model which proved the aforementioned mechanism of delayed vortex formation. He measured the cross-correlation of the longitudinal velocity component along a cylinder using two hot wires located $9D$ behind the cylinder at the edge of the wake. Figure 29 shows that the farwake of the plain model was the least correlated, whilst the farwake behind the model with helical strakes was the best correlated. This indicates that the recovery of the vortex formation process took place furthest downstream for the latter, and is particularly well correlated at the edge of the wake. This piece of information explains why, in the case of two circular cylinders in a tandem arrangement with a spacing between them of $9D$, it was better to leave the upstream cylinder without helical strakes, as found by Walshe and Cowdrey [49]. If both cylinders are fitted with helical strakes, then the downstream one will be exposed to a postponed vortex formation region produced by the upstream cylinder.

The last but not the least factor which should be taken into account in assessing various means is the drag coefficient. It has been pointed out that the effectiveness of the means does not depend on the value of the drag coefficient. A compilation of all available data on drag coefficients for various means is shown in Fig. 30. The helical strakes produce drag in excess of that found for a plain cylinder in the subcritical regime. The perforated shroud with circular holes has the lowest drag whilst the axial-slat shroud produces the highest drag among the shrouds. The means having extremely low drag were guiding vanes in the subcritical regime and helical wires in the critical and supercritical regimes. In general, unidirectional means produced lower drag than omnidirectional means of the same kind.

Acknowledgements

The writer is considerably indebted to a number of people who have provided

data which have been used in this review. Their original papers are cited in the references, and particular mention should be given to the research at the National Physical Laboratory, Teddington, England, headed by Mr. Christopher Scruton, which held a prominent position in the 60's. In addition, the following should be mentioned: Dr. P.W. Bearman of Imperial College, who kindly supplied the unpublished photographs shown in Fig. 26; Prof. M.V. Morkovin of I.I.T. for memorable discussions in Chicago in 1979; Dr. P.K. Stansby, who read and corrected the original manuscript; Mr. D.E.J. Walshe of NMI for many helpful comments; and last but not least, my former students, Mr. D. Postle, Mr. J.R. Volk and Mr. P.J. Southworth, who assisted in the experiments on the axial-rod shroud in the early 70's.

References

1 C. Scruton and A.R. Flint, Wind-excited oscillations of structures, Proc. Inst. Civ. Eng., 27 (1964) 673—702.
2 M.V. Morkovin, Flow around a circular cylinder — a kaleidoscope of challenging fluid phenomena, Am. Soc. Mech. Eng. Symp. on Fully Separated Flow, 1964, pp. 102—118.
3 C. Scruton and E.W.E. Rogers, Wind effects on buildings and other structures, Philos. Trans. R. Soc. London, Ser. A, 269 (1971) 353—383.
4 G.V. Parkinson, Mathematical models of flow-induced vibrations of bluff bodies, in E. Naudascher (Ed.), Flow Induced Structural Vibrations, Springer, Berlin, 1974, pp. 81—122.
5 P.W. Bearman, On vortex shedding from a circular cylinder in the critical regime, J. Fluid Mech., 37 (1969) 577—585.
6 A. Roshko, Experiments on the flow past a circular cylinder at very high Reynolds number, J. Fluid Mech., 10 (1961) 345—356.
7 J.H. Gerrard, An experimental investigation of the oscillating lift and drag of a circular cylinder shedding turbulent vortices, J. Fluid Mech., 11 (1961) 244—256.
8 G.W. Jones, J.J. Cincotta and R.W. Walker, Aerodynamic Forces on a Stationary and Oscillating Circular Cylinder at High Reynolds Numbers, NASA Tech. Rep. R-300 (1969).
9 A. Fage and J.H. Warsap, The effects of turbulence and surface roughness on drag of a circular cylinder, Br. Aerodyn. Res. Counc., Rep. Memo. 1283 (1929).
10 E. Achenbach, Influence of surface roughness on the cross flow around a circular cylinder, J. Fluid Mech., 46 (1971) 321—335.
11 L.R. Wootton, The oscillations of large circular stacks in wind, Proc. Inst. Civ. Eng., 43 (1969) 573—598.
12 G.H. Toebes, The unsteady flow and wake near an oscillating cylinder, Trans. Am. Soc. Mech. Eng., J. Basic Eng., 91 (1969) 493—505; Discuss., 859—862.
13 R. King, A review of vortex shedding research and its application, Ocean Eng., 4 (1977) 141—172.
14 G.W. Parkinson, Wind induced instability of structures, Philos. Trans. R. Soc. London, Ser. A, 269 (1971) 395—409.
15 D.E. Walshe and L.R. Wootton, Preventing wind-induced oscillations of structures of circular section, Proc. Inst. Civ. Eng., 47 (1970) 1—24.
16 M.M. Zdravkovich, Variation on the theme of mechanics of vortex shedding, Euromech Colloq. 119, Imperial College, London, 1979; see also, Phenomenological concepts of vortex shedding and related phenomena. J. Fluid Mech., submitted for publication.
17 C. Scruton and D.E.J. Walshe, A means for avoiding wind-excited oscillations of structures with circular or nearly circular cross section, Natl. Phys. Lab. (U.K.), Aero Rep.

335 (1957); Br. Pat. 907,851; see also, C. Scruton, Note on a device for the suppression of the vortex excited oscillations of flexible structures of circular or near circular section, with special reference to its application to tall stacks, Natl. Phys. Lab. (U.K.), Aero Note 1012 (1963).
18 K. Nakagawa, Ts. Fujino, Y. Arita, Y. Ogata and K. Masaki, An experimental investigation of aerodynamic instability of circular cylinders at supercritical Reynolds numbers, Proc. 9th Jpn. Congr. Appl. Mech., Tokyo, 1959, pp. 235—240.
19 M. Novak, The wind induced lateral vibration of circular guyed masts, tower-shaped steel and reinforced concrete structures, Symp. Int. Ass. Shell Struct., Bratislava, 1966; see also, Int. Res. Semin. on Wind Effects on Buildings and Structures, Ottawa, 1967, Vol. 2, pp. 429—457.
20 D.W. Sallet and J. Berezow, Suppression of flow-induced vibrations by means of body surface modifications, Shock Vib. Bull., Nav. Res. Lab., Washington, DC, 42 (1972) 215—228.
21 P. Price, Suppression of the fluid-induced vibration of circular cylinders, Proc. Am. Soc. Civ. Eng., J. Eng. Mech. Div., 82 (1956) pap. 1030.
22 A. Naumann, M. Morsbach and C. Kramer, The conditions of separation and vortex formation past cylinders, AGARD Conf. Pap. 4 (1966) 539—574.
23 M. Alexandre, Experimental study of the action of vortex shedding on cylinders with longitudinally welded fins, paper presented at Euromech Colloq. 17, 1970, Cambridge (U.K.); see W.A. Mair and D.J. Maull, Bluff bodies and vortex shedding: a report on Euromech 17, J. Fluid Mech., 45 (1971) 209—223; see also, A. Vandeghem and M. Alexandre, Vibration des grandes cheminees en acier sons l'action du vent, Int. Ass. Bridge and Struct. Eng., Publ. 20-I (1969).
24 Sh. Mizuno, Effects of three-dimensional roughness elements on the flow around a circular cylinder, J. Sci. Hiroshima Univ., Ser. A-II, 34 (1970) 214—258.
25 K. Nakagawa, Ts. Fujino, Y. Arita and K. Shima, An experimental study of aerodynamic devices for reducing wind-induced oscillatory tendencies of stacks, in C. Scruton (Ed.), Wind Effects on Buildings and Structures, Symp. Natl. Phys. Lab. (U.K.), Teddington, 1963, H.M.S.O., 1965, pp. 774—795.
26 O. Mahrenholtz and H. Bardowicks, Aeroelastic problems of masts and chimneys, in C. Kramer and H.J. Gerhardt (Eds.), Proc. 3rd Colloq. on Industrial Aerodynamics, Aachen, 1978, Part 2, pp. 35—47.
27 I.S. Gartshore, J. Khanna and S. Laccinole, The effectiveness of vortex spoilers on a circular cylinder in smooth and turbulent flow, Proc. 5th Int. Conf. on Wind Engineering, Fort Collins, CO, 1978.
28 M.M. Zdravkovich and J.R. Volk, Effect of shroud geometry on the pressure distribution around a circular cylinder, J. Sound Vib., 20 (1972) 451—455.
29 M.M. Zdravkovich, Circular cylinder enclosed in various shrouds, Am. Soc. Mech. Eng. Vibration Conf., Toronto, 1971, Pap. 71-VIBR-28; U.K. Pat. Appl. 40768/71.
30 M.M. Zdravkovich, Flow induced vibrations in irregular tube bundles, and their suppression, Proc. Int. Symp. on Vibration Problems in Industry, UKAEA and Natl. Phys. Lab. (U.K.), 1973, Pap. 413.
31 H.Y. Wong, An aerodynamic means of suppressing vortex induced oscillations, Proc. Inst. Civ. Eng., 63 (1977) 693—699.
32 R.C. Baird, Wind-induced vibration of a pipe-line suspension bridge and its cure, Trans. Am. Soc. Mech. Eng., 77 (1955) 797—804.
33 A. Roshko, On the wake and drag of bluff bodies, J. Aeronaut. Sci., 22 (1955) 124—132.
34 G. Grimminger, The effect of rigid guide vanes on the vibration and drag of a towed circular cylinder, David Taylor Model Basin, Washington, Rep. 504 (1945).
35 C.J. Wood, The effect of base bleed on a periodic wake, J. R. Aeronaut. Soc., 68 (1964) 477—482.
36 T. Igarashi, Flow characteristics around a circular cylinder with a slit, Bull. Jpn. Soc. Mech. Eng., 21 (1978) 656—664.

37 L. Prandtl, Gottinger Nachrichten, (1914) 177—190; see also, C. Wieselsberger, Drag of spheres, Z. Flugtech. Motorluft Schiff., 5 (1914) 140—144 (in German).
38 D.F. James and Q.S. Truong, Wind load on cylinder with spanwise protrusion, Proc. Am. Soc. Civ. Eng., J. Eng. Mech. Div., 98 (1972) 1573—1589.
39 L. Woodgate and J.F.M. Maybrey, Further experiments on the use of helical strakes for avoiding wind excited oscillations of structures of circular or nearly circular section, Natl. Phys. Lab. (U.K.), Aero Rep. 381 (1959).
40 C.F. Cowdrey and J.A. Lawes, Drag measurements at high Reynolds numbers of a circular cylinder fitted with three helical strakes, Natl. Phys. Lab. (U.K.), Aero Rep. 384 (1959).
41 H. Ruscheweyh, Tip effect on vortex excited oscillation of a model stack with and without efflux stream, Symp. on Flow Induced Structural Vibrations, Karlsruhe, W. Germany, 1972, Suppl., 101—103 (not published in the Proceedings).
42 B.J. Vickery and R.D. Watkins, Flow induced vibrations of cylindrical structures, in R. Silvester (Ed.), Proc. 1st Aust. Conf. on Hydraulics and Fluid Mechanics, Pergamon, 1964, pp. 213—241.
43 W. Weaver, Wind-induced vibrations in antenna members, Proc. Am. Soc. Civ. Eng., J. Eng. Mech. Div., 87 (1961) 141—165.
44 M.M. Zdravkovich and G.L. Hodge, The disappearance of the wake shock behind a cylinder in a supersonic flow at high Reynolds number, Trans. Am. Soc. Mech. Eng., J. Fluid Eng., 97 (1975) 120—122.
45 D.E.J. Walshe, Wind tunnel investigation of the dynamic behaviour of some tall stacks and gas turbine exhaust towers, in D.J. Johns, C. Scruton and A.M. Ballantyne (Eds.), Proc. Symp. on Wind Effects on Building and Structures, Loughborough University, 1968, Pap. 17.
46 B.J. Knell, The drag of a circular cylinder fitted with shrouds, Natl. Phys. Lab. (U.K.), Aero Rep. 1297 (1969).
47 L.R. Wootton and D. Yates, Further experiments on drag of perforated shrouds, Natl. Phys. Lab. (U.K.), Aero Rep. 1321 (1970).
48 R.E.F. Gould, W.G. Raymer and P.J. Ponsford, Wind tunnel tests on chimneys of circular cross section at high Reynolds numbers, in D.J. Johns, C. Scruton and A.M. Ballantyne (Eds.), Proc. Symp. on Wind Effects on Buildings and Structures, Loughborough University, 1968, Pap. 10; see also, Natl. Phys. Lab. (U.K.), Aero Rep. 1266 (1968).
49 D.E. Walshe and C.F. Cowdrey, A brief study of the effect of shrouds on buffet amplitudes of chimney stacks, Natl. Phys. Lab. (U.K.), Maritime Sci. Tech. Memo. 2-72 (1972).
50 G.M. Moss, Oscillations induced by a shallow cylindrical element on a tall tower, in D.J. Johns, C. Scruton and A.M. Ballantyne (Eds.), Proc. Symp. on Wind Effects on Buildings and Structures, Loughborough University, 1968, Pap. 2.
51 M.S. Ozker and J.O. Smith, Factors influencing the dynamic behaviour of tall stacks under the action of the wind, Trans. Am. Soc. Mech. Eng., 78 (1956) 1381—1391.
52 M.M. Zdravkovich, Smoke observations of the wake of a group of three cylinders at low Reynolds number, J. Fluid Mech., 32 (1968) 339—351.
53 M.M. Zdravkovich and J.E. Namork, Excitation and amplification of flow induced vibration in compact heat exchangers, in E. Naudascher and D. Rockwell (Eds.), Practical Experience with Flow Induced Vibrations, Springer, Berlin, 1980, pp. 109—117.
54 P.W. Bearman and M.M. Zdravkovich, Flow around a circular cylinder near a plane boundary, J. Fluid Mech., 89 (1978) 33—47.
55 M.M. Zdravkovich and P.J. Southworth, Effect of shroud eccentricity on suppression of flow induced vibrations, J. Sound Vib., 27 (1973) 77—84.

56 M.M. Zdravkovich, Flow induced vibrations of two cylinders in tandem, and their suppression, in E. Naudascher (Ed.), Flow Induced Structural Vibrations, Springer, Berlin, 1974, pp. 631—639.
57 H.Y. Wong, A means of controlling bluff body flow separation, J. Ind. Aerodyn., 4 (1979) 183—201.
58 R. King, Troubleshooting offshore, Br. Hydraul. Res. Ass., Newslett. No. 30 (1979).
59 S.F. Hoerner, Aerodynamic Drag (1951, 1958) and Fluid Dynamic Drag (1965) (published by the author); 3-2, Fig. 1-D; 3-7, Fig. 8.
60 A. Roshko, On the drag and shedding frequency of two-dimensional bluff bodies, Natl. Adv. Comm. Aeronaut. Tech. Note 3169 (1954).
61 P.W. Bearman, Investigation of the flow behind a two dimensional model with a blunt trailing edge and fitted with splitter plates, J. Fluid Mech., 21 (1965) 241—255.
62 A. Roshko, On the development of turbulent wakes from vortex streets, Natl. Adv. Comm. Aeronaut., Tech. Rep. 1191 (1954).
63 R. Parker, Resonance effects in wake shedding from parallel plates, J. Sound Vib., 4 (1966) 62—72; 5 (1967) 330—343.
64 M. Gaster, Some observations on vortex shedding and acoustic resonances, Br. Aeronaut. Res. Counc., Curr. Pap. 1141 (1970); see also, Natl. Phys Lab. (U.K.), Aero Rep. 1311 (1970).
65 D.W. Sallet, On the reduction and prevention of the fluid induced vibrations of circular cylinders of finite length, Shock Vib. Bull., Nav. Res. Lab., Washington, DC, 41 (1970) 31—37.
66 D.W. Sallet, A method of stabilizing cylinders in fluid flow, J. Hydronaut., 4 (1970) 40—45.
67 C.J. Appelt, G.S. West and A.A. Szewczyk, The effects of wake splitter plates on the flow past a circular cylinder in the range $10^4 < Re < 5 \times 10^5$, J. Fluid Mech., 61 (1973) 187—198; 71 (1975) 145—160.
68 C.J. Wood, The effect of lateral vibrations on vortex shedding from blunt based aerofoils, J. Sound Vib., 14 (1971) 91—102.
69 J.H. Gerrard, The mechanics of the formation region of vortices behind bluff bodies, J. Fluid Mech., 25 (1966) 401—413.
70 C.J. Wood, Visualization of an incompressible wake with base bleed, J. Fluid Mech., 29 (1967) 259—272.
71 S. Taneda, Downstream development of the wakes behind cylinders, J. Phys. Soc. Jpn., 14 (1959) 843—848.
72 A.R.J. Borges, On wind induced instability of television towers, Proc. Int. Conf. on Wind Effects on Buildings and Structures, Tokyo, 1971, pp. 1101—1110.